



**DEVELOPMENT PATH PLANNING OF WIRE ARC ADDITIVE  
MANUFACTURING ROBOTIC SYSTEM BASED ON OPEN-  
SOURCE SOFTWARE**



**BACHELOR OF MECHANICAL ENGINEERING TECHNOLOGY  
WITH HONOURS**

**2024**



## **Faculty of Mechanical Technology and Engineering**

A faded version of the UTeM logo and university name is visible in the background behind the title text.

# **DEVELOPMENT PATH PLANNING OF WIRE ARC ADDITIVE MANUFACTURING ROBOTIC SYSTEM BASED ON OPEN-SOURCE SOFTWARE**

Muhammad Nor Haikal bin Noor Aziz

**Bachelor of Mechanical Engineering Technology with Honours**

2024

**DEVELOPMENT PATH PLANNING OF WIRE ARC ADDITIVE  
MANUFACTURING ROBOTIC SYSTEM BASED ON OPEN-SOURCE  
SOFTWARE**

**MUHAMMAD NOR HAIKAL BIN NOOR AZIZ**



**Faculty of Mechanical Technology and Engineering**

**UNIVERSITI TEKNIKAL MALAYSIA MELAKA**

**2024**

**BORANG PENGESAHAN STATUS LAPORAN PROJEK SARJANA MUDA**

**TAJUK: DEVELOPMENT PATH PLANNING OF WIRE ARC ADDITIVE MANUFACTURING ROBOTIC SYSTEM BASED ON OPEN-SOURCE SOFTWARE**

SESI PENGAJIAN: **2023-2024 Semester 1**

Saya **MUHAMMAD NOR HAIKAL BIN NOOR AZIZ**

mengaku membenarkan tesis ini disimpan di Perpustakaan Universiti Teknikal Malaysia Melaka (UTeM) dengan syarat-syarat kegunaan seperti berikut:

1. Tesis adalah hak milik Universiti Teknikal Malaysia Melaka dan penulis.
2. Perpustakaan Universiti Teknikal Malaysia Melaka dibenarkan membuat salinan untuk tujuan pengajian sahaja dengan izin penulis.
3. Perpustakaan dibenarkan membuat salinan tesis ini sebagai bahan pertukaran antara institusi pengajian tinggi.
4. **\*\*Sila tandakan (✓ )**

- TERHAD** (Mengandungi maklumat yang berdarjah keselamatan atau kepentingan Malaysia sebagaimana yang termaktub dalam AKTA RAHSIA RASMI 1972)
- SULIT** (Mengandungi maklumat TERHAD yang telah ditentukan oleh organisasi/badan di mana penyelidikan dijalankan)
- TIDAK TERHAD**

Disahkan oleh:



Alamat Tetap:

Lot 61A, Rumah 12, Batu Empat  
Setengah, Kampung Pasir,  
34600, Kamunting, Perak

Tarikh: 12/1/2024



**DR. NOR ANA BINTI ROSLI**  
Pensyarah  
Jabatan Teknologi Industri  
Fakulti Teknologi Kejuruteraan Mekanikal  
dan Pembuatan (FTKMP)  
Universiti Teknikal Malaysia Melaka

Cop Rasmi:

Tarikh: \_\_\_\_\_

**\*\* Jika tesis ini SULIT atau TERHAD, sila lampirkan surat daripada pihak berkuasa/organisasi berkenaan dengan menyatakan sekali sebab dan tempoh laporan PSM ini perlu dikelaskan sebagai SULIT atau TERHAD.**

## DECLARATION

I declare that this Choose an item. entitled “**DEVELOPMENT PATH PLANNING OF WIRE ARC ADDITIVE MANUFACTURING ROBOTIC SYSTEM BASED ON OPEN-SOURCE SOFTWARE**” is the result of my own research except as cited in the references. The Choose an item. has not been accepted for any degree and is not concurrently submitted in candidature of any other degree.

Signature

:



Name

:

MUHAMMAD NOR HAIKAL BIN NOOR AZIZ

Date

:

12 JANUARY 2024



اونيورسيتي تيكنيكا ماليسيا ملاك

UNIVERSITI TEKNIKAL MALAYSIA MELAKA

## APPROVAL

I hereby declare that I have checked this thesis and in my opinion, this thesis is adequate in terms of scope and quality for the award of the Bachelor of Mechanical Engineering Technology with Honours.

Signature :



Supervisor Name : DR ANA BINTI ROSLI

12 JANUARY 2024

Date :



اونيورسيتي تيكنيكل مليسيا ملاك

UNIVERSITI TEKNIKAL MALAYSIA MELAKA

## DEDICATION

This report is dedicated to my family, whose unwavering support and love have been my driving force throughout this journey. Your support and confidence in my abilities have motivated me to exceed my limits and pursue excellence. Thank you for always being there for me, encouraging me on and creating an environment helpful to my personal and academic development. Dr. Ana binti Rosli, my project's supervisor, has provided me with invaluable guidance, expertise and unwavering dedication to the success of my project. Your insightful feedback, patience and encouragement have been vital in shaping my research and challenging me to perform at my highest level. My classmates and friends have been an incredible source of support and companionship throughout the duration of this work. Your enthusiasm, ideation sessions and willingness to lend a hand have enhanced the value of this experience. I would also like to thank the Faculty of Technology at Universiti Teknikal Malaysia Melaka for providing the necessary resources, facilities and opportunities that have facilitated the completion of this undertaking. Your dedication to academic excellence and research has significantly contributed to my growth as a student and researcher. Lastly, I would like to thank all who has directly or indirectly taking part to the successful completing this endeavour. Your encouragement, belief in my abilities and support have fueled my resolve and enabled me to overcome obstacles along the way. May Allah always bless of them.

## ABSTRACT

Wire arc additive manufacturing (WAAM) is one of the types additive manufacturing (AM) that uses the arc welding as the heating source and metal wire as the feedstock. Wire arc additive manufacturing (WAAM) is an additive manufacturing process utilizing arc welding and metal wire, showing promise for cost-effective and quick manufacture of large-scale metal structures. Despite its advantages, issues in controlling robot motions and designing welding torch trajectories continue. Researchers commonly adapt CNC machining G code for tool feed trajectory to fit welding gun action, utilizing programs like "MasterCAM" transformed by "Robotmaster" or "3D Automate." This work provides an alternate way to enhance flexibility and reliability in path planning for WAAM leveraging robot-based production of CAD files as a result, path planning for WAAM is based on open-source software such as "Cura" slicing software had been developed and the 3D model structure had been fabricated. The goal is to determine the path planning of wire arc additive manufacturing. To construct 3D model using robotic based on WAAM to establish the path planning and optimal parameter has been discovered. The path planning had been developed via slicer and compare it with the other framework to prove as proof for aim one achieved. Two parameters were employed based on past research to establish the appropriate parameter to apply in manufacture of complex model. The result of the parameter chosen were influenced the structure and the manufacturing of model. As conclusion, these objectives were achieved due to the prove of the complex model outcome.

اونيورسيتي تيكنيكل مليسيا ملاك

UNIVERSITI TEKNIKAL MALAYSIA MELAKA

## ***ABSTRAK***

Salah satu jenis additive manufacturing (*AM*), wire arc additive manufacturing (*WAAM*), menggunakan arc welding sebagai sumber pemanasan dan wayar besi sebagai bahan mentah. Wire arc additive manufacturing (*WAAM*) adalah proses pembuatan tambahan yang menggunakan pengelasan busur dan kawat logam, menunjukkan potensi untuk pembuatan struktur logam skala besar yang hemat biaya dan cepat. Meskipun memiliki keunggulan, masalah dalam mengendalikan gerakan robot dan merancang lintasan obor pengelasan masih ada. Para peneliti umumnya mengadaptasi kode G mesin CNC untuk lintasan umpan alat agar sesuai dengan aksi pistol pengelasan, dengan menggunakan program seperti "*MasterCAM*" yang diubah oleh "*Robotmaster*" atau "*3D Automate*". Karya ini menyediakan cara alternatif untuk meningkatkan fleksibilitas dan keandalan dalam perencanaan lintasan untuk *WAAM* dengan memanfaatkan produksi berbasis robot dari file CAD. Sebagai hasilnya, perencanaan lintasan untuk *WAAM* didasarkan pada perangkat lunak sumber terbuka seperti perangkat lunak pemotongan "*Cura*" yang telah dikembangkan dan struktur model 3D telah difabrikasi. Tujuannya adalah untuk menentukan perencanaan lintasan dari wire arc additive manufacturing. Untuk membangun model 3D menggunakan robot berbasis *WAAM* untuk menetapkan perencanaan lintasan dan parameter optimal telah ditemukan. Perancangan laluan dibuat melalui pemotongan dan dibandingkan dengan rangka kerja lain untuk menunjukkan pencapaian objektif pertama. Dua parameter yang sesuai telah diwujudkan berdasarkan penyelidikan terdahulu untuk pembuatan model yang kompleks. Parameter yang dipilih mempengaruhi struktur dan penghasilan model. Kesimpulannya, semu objektif telah dicapai disebabkan penghasilan keputusan model kompleks.

اويور سيتي تيكنيكل مليسيا ملاك

UNIVERSITI TEKNIKAL MALAYSIA MELAKA

## ACKNOWLEDGEMENTS

In the Name of Allah, the Most Gracious, the Most Merciful

The completion of this thesis is a tribute to Allah and His grace. I give thanks to God for all the chances, difficulties, and resources that have enabled me to complete the thesis. Throughout this process, I learned a great deal about myself on both an academic and a personality level. I owe the sincerest thanks to the holy Prophet Muhammad (Peace be upon him), whose example of living has provided me with constant direction. My supervisor, Dr Ana binti Rosli, deserves special thanks for his guidance and unwavering support. The success of this study has been attributed to her great assistance with constructive criticism and ideas throughout the experimental and thesis activities. Sincere appreciation to all my friends, especially for your generosity and encouragement while I was studying. My sincere appreciation also extends to my dear parents for their unending support, prayers, and love. It means a lot to me that you helped with this final year project in an indirect way. I appreciate you.

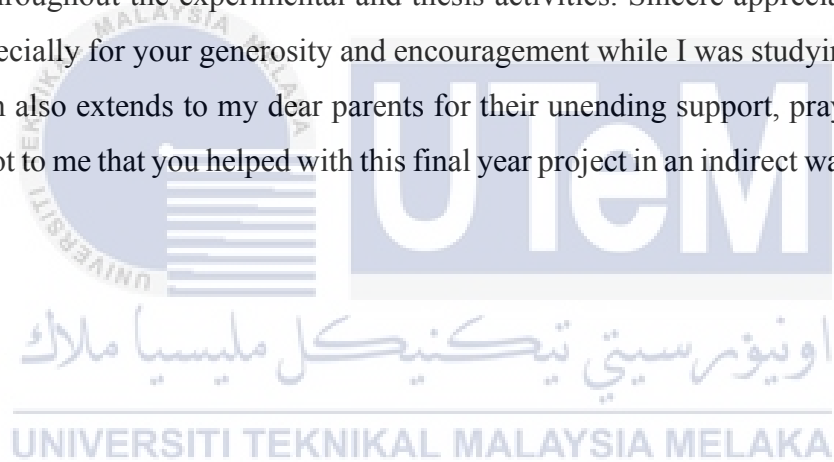


## TABLE OF CONTENTS

	PAGE
<b>DECLARATION</b>	
<b>APPROVAL</b>	
<b>DEDICATION</b>	
<b>ABSTRACT</b>	ii
<b>ABSTRAK</b>	iii
<b>ACKNOWLEDGEMENTS</b>	iv
<b>TABLE OF CONTENTS</b>	v
<b>LIST OF TABLES</b>	vii
<b>LIST OF FIGURES</b>	viii
<b>LIST OF SYMBOLS AND ABBREVIATIONS</b>	x
<b>LIST OF APPENDICES</b>	xi
<b>CHAPTER 1 INTRODUCTION</b>	<b>1</b>
1.1 Background	1
1.2 Problem Statement	4
1.3 Research Objective	1
1.4 Scope of research	1
1.5 Organization	1
<b>CHAPTER 2 LITERATURE REVIEW</b>	<b>3</b>
2.1 Introduction of Additive Manufacturing (AM)	3
2.2 Wire Arc Additive Manufacturing (WAAM) and Robotics	5
2.2.1 Working principle of Wire Arc Additive Manufacturing	7
2.2.2 Types of principle in Wire Arc Additive Manufacturing (WAAM)	8
2.3 Principle of MIG-WAAM	9
2.4 Principle of CMT Technology	10
2.5 Principle of TIG-WAAM	12
2.6 Principle of PAW-WAAM	13
2.7 Robotic motion mechanism	15
2.8 Six joint axes robotic mechanism	16
2.9 3D printing robotic mechanism	17
2.10 Material description and Welding Consumable	18
2.11 Open-source software for WAAM	22
2.12 Welding Parameter	24
2.13 Cooling rate	28
2.14 Welding Imperfection and defects	30

2.14.1	Excessive heat	31
2.14.2	Porosity/ Gas bubble	32
2.14.3	Overlap	33
2.14.4	Lack of fusion	34
<b>CHAPTER 3</b>	<b>METHODOLOGY</b>	<b>36</b>
3.1	Introduction	36
3.2	Gantt Chart	36
3.3	Progress flowchart	37
3.4	Wire arc additive manufacturing process	38
3.5	Equipment used.	39
3.6	Path planning flow for robot WAAM	40
3.6.1	Parameter in the “Cura” software printing setting.	41
3.7	Fabrication of 3D structure	46
3.7.1	Design of 3D model	46
3.7.2	Material preparation	46
3.7.3	Fit Up process.	47
3.7.4	Machine preparation	48
3.7.5	Welding process	49
3.7.6	Pre-cleaning	50
3.7.7	Observation method	50
<b>CHAPTER 4</b>	<b>RESULTS AND DISCUSSION</b>	<b>52</b>
4.1	Introduction	52
4.2	Printing setting path planning flow for robot WAAM	52
4.3	Single layer deposition.	55
4.3.1	Result of the fabrication of the single line layer.	55
4.3.2	Coding for single line based on the slicer model.	56
4.3.3	Command of controller robot welding arm.	56
4.3.4	Comparison of the command of the robot welding arm.	57
4.3.5	Analysis of single layer deposition.	58
4.3.6	Observation Test Result	58
4.3.7	Observation test for parameter A.	59
4.3.8	Observation test for parameter B	60
4.3.9	Overall summary of the two parameters	61
4.3.10	Chosen of optimal parameter of single layer deposition.	62
4.4	Fabrication of the 3D complex model.	63
4.4.1	Coding for the complex model	64
4.4.2	Command of the robot welding for complex model.	64
4.4.3	Discussion and evaluation of the 3D complex model.	65
<b>CHAPTER 5</b>	<b>CONCLUSION AND RECOMMENDATIONS</b>	<b>66</b>
5.1	Conclusion	66
5.2	Recommendations	66
5.3	Project Potential	67
<b>REFERENCES</b>		<b>69</b>
<b>APPENDICES</b>		<b>74</b>

## LIST OF TABLES

TABLE	TITLE	PAGE
Table 1:	List of tensile test material Stainless steel and carbon steel, Source (S.I. Evans et al, 2022)	19
Table 2:	Chemical Composition of material (wt.-%), Source (A.Ermakova et al, 2020)	22
Table 3:	Factors and level for the welding process, source (Diah Kusuma Pratiwi ,2023)	27
Table 4:	Experimental layout and factor distribution of the orthogonal array (L9), source (Diah Kusuma Pratiwi ,2023)	28
Table 5:	Chemical composition of the ER70S-6 wire in weight percentage(%), source (Merbin et al., 2021)	49
Table 6:	Comparison of the command robot welding	57
Table 7:	Analysis of dingle line layer deposition parameters.	58
Table 8:	Welding parameter of Parameter A	59
Table 9:	Welding parameter of parameter B	60
Table 10:	Table of the welding defects with the Visual result	61
Table 11:	Best selection of the parameter for single line layer	62

## LIST OF FIGURES

<b>FIGURE</b>	<b>TITLE</b>	<b>PAGE</b>
Figure 1.1:	Trend journals published about AM (database from Scopus)	2
Figure 1.2:	Types of metal AM techniques, source (Alkahari M et al, 2021)	3
Figure 2.1:	Working principle of WAAM, source (Anthony R. McAndrew et al, 2018)	8
Figure 2.2:	Principle of MIG, source (Ding et al., 2015)	10
Figure 2.3:	A process of CMT method of surfacing by welding, source (Słania et al,2015)	12
Figure 2.4:	Principle of TIG , source (Ding et al., 2015)	13
Figure 2.5:	Principle of TIG-WAAM, Source (D.H.Ding et al, 2015)	15
Figure 2.6:	Six axis of robotic arm, source (Rambod Rastegari, 2016)	17
Figure 2.7:	3D printing with X, Y and Z axis label, source (A.Munaz et al, 2016)	18
Figure 2.8:	Welding condition, source (S. Srivastava,2020)	26
Figure 2.9:	Classification of distortion, source (Zuheir Barsoum,2015)	31
Figure 2.10:	Porosity while running experiment, source (T. Hauser et al., 2021)	33
Figure 2.11:	The schematic of overlap, source (Blockadvtech, 2018)	34
Figure 2.12:	Schematic of lack of fusion, souce (Blockadvtech, 2018)	35
Figure 3.1:	Research flow Chart	37
Figure 3.2:	Wire arc additive manufacturing system	38
Figure 3.3:	Slicing process using “Cura” slicing software	41
Figure 3.4:	Parameter of each layer height, thickness and wall thickness	42

Figure 3.5: Parameter of Infill density and temperature of printing	43
Figure 3.6: Parameter of the speed and travel printing	44
Figure 3.7: Parameter of cooling section printing	45
Figure 3.8: The model after slicing begins and path planning shown	45
Figure 3.9: 3D model structures with dimensions	46
Figure 3.10: Material preparation (Mild steel plate)	47
Figure 3.11: Overview of substrate plate fit up process with dimension	47
Figure 3.12: Wire feeder unit Copper coated ER70S-6 Ø 1.0 mm	48
Figure 3.13: IRB 1410 M2004 robot welding	49
Figure 4.1: Path planning result for slicer.	54
Figure 4.2: Different framework of the single line model	56
Figure 4.3: Picture of the welding parameter A	59
Figure 4.4: Picture of the welding parameter B	61
Figure 4.5: Framework of the complex model	63
Figure 4. 6: Fabrication of complex model	64

## LIST OF SYMBOLS AND ABBREVIATIONS

AM	-	Additive Manufacturing
WAAM	-	Wire Arc Additive Manufacturing
SLM	-	Selective Laser Melting
LMD	-	Laser Metal Deposition
EBM	-	Electron Beam Melting
WLAM	-	Wire And Laser Additive Manufacturing
EBF <sup>3</sup>	-	Electron Beam Freeform Fabrication
LENS	-	Laser Engineered Net Shaping
3D	-	Three-dimensional
OSS	-	Open-Source Software
MIG	-	Metal Inert GAs
GMAW	-	Gas Metal Arc Welding
CMT	-	Cold Metal Transfer
TIG	-	Tungsten Inert Gas
PAW	-	Plasma Arc Welding
UTS	-	Ultimate Tensile Strength
HV	-	High Voltage
CAD	-	Computer Aided Design
CFD	-	Computational Fluid Dynamics
SMAW	-	Shielded Metal Arc Welding
DSS	-	Duplex Stainless Steel
CO <sub>2</sub>	-	Carbon Dioxide

## LIST OF APPENDICES

APPENDIX	TITLE	PAGE
APPENDIX A:	Gantt Chart	74
APPENDIX B:	Coding for single line layer	75
APPENDIX C:	Command A for single line layer	76
APPENDIX D:	Command B for single layer	77
APPENDIX E:	Command for complex model	78
APPENDIX F:	Turnitin Report Result	81



# CHAPTER 1

## INTRODUCTION

The background study, problem statement, objectives, scope and organization are all included in this chapter. The chapter explains the major introduction of the objective of performing this project and insight into how the concept is formed.

### 1.1 Background

According to Chen et al., (2023), in the field of worldwide advanced manufacturing, additive manufacturing (AM) sometimes referred to as 3D printing is a promising bottom-up (layer-by-layer) forming method that integrates equipment, computers, numerical control and materials. It can quickly fabricate parts with complex structures utilizing a various of metal materials, non-metal materials or medicinal biomaterials compatible with the discrete-stacking principle since it is based on digital three-dimensional modelling (Chen C et al, 2022). Many methods can be used to add the material including extrusion, welding, curing, inkjet deposition and others. The main benefit of additive manufacturing over traditional subtractive manufacturing is that it has freed the designer from most manufacturing restrictions. Additionally, the technology excuses manufacturers from performing simple assembly tasks and traditional tooling. Many industries, including aerospace, defence, automotive and medical devices have begun to utilize AM technology. The need to automate machine operation, decrease waste material, minimize energy usage and enhance material efficiency encourages the use of additive manufacturing. Industrial and most academia have shown a great interest in the potential of Additive Manufacturing. Scopus database estimate from 2016 states that AM

produced 2648 journals in that year. Until recently, it was predicted that this scope journal would increase to 3651 by 2017, 5058 by 2018, 6444 by 2019, 8237 by 2020, 9342 by 2021 and exceed to 10808 by 2022, with 4304 journals being produced in 2023. These figures 1.1 describe journals that have been published since 2016 up to the present.

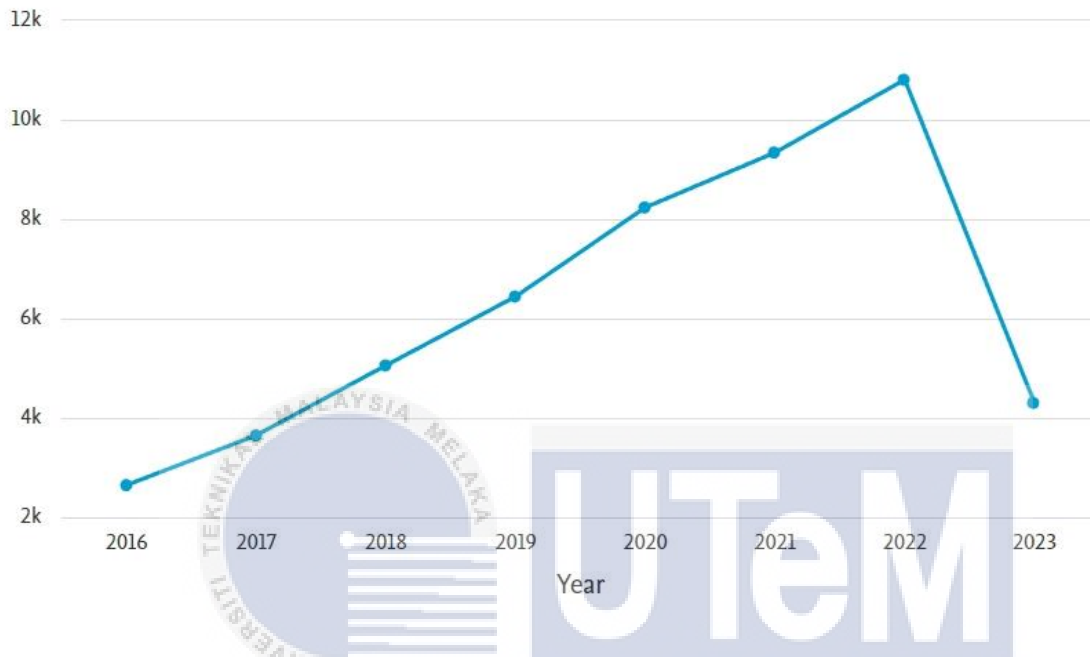


Figure 1.1: Trend journals published about AM (database from Scopus)

Along with that, the capability of AM to produce free form components layer by layer and in three dimensions is a main reason for advancements. Powder-based and wire-based are the two types of metal structure AM. In powder based, the metallic powder is melting using a laser beam or an electron beam such as selective laser melting (SLM), laser metal deposition (LMD) and electron beam melting (EBM) process (Leitz et al., 2017). Regarding wire-based manufacturing, instead of using metal powder, wire is used and is melted using a laser, electron beam, or electric arc. These processes embrace wire and laser additive manufacturing (WLAM), electron beam freeform fabrication (EBF<sup>3</sup>), Laser Engineered Net Shaping (LENS) and wire arc additive manufacturing (WAAM). Figure 1.2 represents the types of metal of additive manufacturing below.

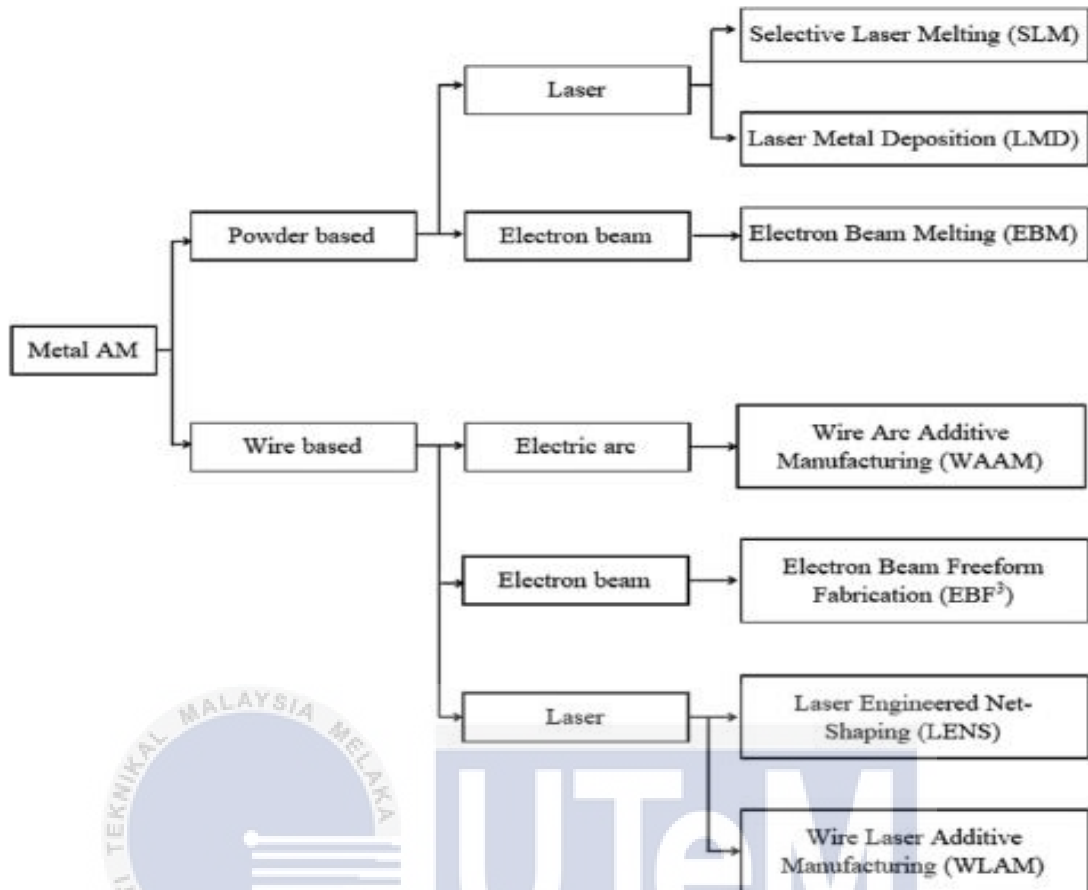


Figure 1.2: Types of metal AM techniques, source (Alkahari M et al, 2021)

Due to capacity to produce large scale metal components with a high deposition rate, low-cost material, high material consumption and consequent environmentally friendly, wire arc additive manufacturing (WAAM) has gained popularity in the industrial manufacturing industry in recent years (Snider-Simon & Frantziskonis, 2022). These innovations and variations are becoming more widespread in our culture. While minimizing the environmental impact of the production and repair of these components, it is occasionally necessary to repair damaged components and produce geometrically complex components. Using additive manufacturing could answer the growing environmental concerns and the demand for more effective resource management in the manufacturing industry. The WAAM process was the best choice for this development because of its simplicity and adaptability (Derekar, 2018).

Despite its many benefits, WAAM still has a lot of work to do, especially when designing the path for moving the welding flame and effectively controlling the robot's movement. Traditional path planning and control techniques are frequently ineffective and time-consuming, which increases expenses and decreases production. There is a need for an alternate method that can increase the path planning system's dependability and flexibility in order to fully utilize the potential of WAAM.

## 1.2 Problem Statement

Wire arc additive manufacturing (WAAM) is one of the additive manufacturing (AM) techniques that use arc welding as the heat source and metal wire as the raw material. The WAAM technique holds promise for producing large-scale metal structures at low cost and high deposition speeds. Due to its benefit, the largest demand for WAAM has come from business and academia. Compared to other metal AM techniques, WAAM is more affordable, has less material waste, and requires less production time. However, one of the major difficulties WAAM faces is to control the robot movement and planning the path for the welding torch using arc welding as heat source. In additive manufacturing requires careful design of the welding torch movement route and efficient control based on layered slicing of the 3D model. Many researchers transform the CNC machining G code, changing the tool feed trajectory to the welding gun movement trajectory to use CNC machine tools and other processing platforms. Much research uses CNC machining programmes like “MasterCAM”, which generates G code before being converted by “Robotmaster” or “3D Automate”. In order to make the CAD file compatible with fabrication utilizing a robot based WAAM method, this study suggests an alternate technique that increases the flexibility and reliability of path planning.

### 1.3 Research Objective

- a. To develop the printing setting path planning flow for robot wire arc additive manufacturing (WAAM).
- b. To choose the optimal parameter of single layer deposition using path planning flow of WAAM process
- c. To evaluate the performance of robotic WAAM in fabricating three-dimensional metallic structure.

### 1.4 Scope of research

The scope has been divided into 3 categories which is:

- a. This study majority focus on wire arc additive manufacturing process such as robot welding (ABB IR1410 M2004) types.
- b. For the materials, copper wire ER70S-6 was used as feedstock for robot welding to build the three-dimensional model structure that had been drawn.
- c. For the mechanism, “Cura” software were used as slicer and path planning method for this study.

### 1.5 Organization

The order of the contents of this chapter is as follows. Chapter one of the research study includes a discussion of the background study, problem statement, objectives and research scope. The second chapter describes the literature review of the research within the parameters involved and serves as the foundation for further discussion in the subsequent section. The third chapter discusses producing G-code using the “Cura” software and determining whether or not robot welding systems like ABB robot welding can read the G-code. The outcome of the constructing of the complex model has been explained in chapter four. In chapter five, the parameter's conclusion, recommendations, and explanation of the results are discussed,

specifically addressing whether the objective was achieved or not. Several different kinds of additive manufacturing exist, including both non-metal and metal-based techniques. These studies focus on the Wire Arc Additive Manufacturing (WAAM) of metal-based goods due to its cost-effectiveness, reduced waste generation, and shorter production time. Wire arc additive manufacturing requires extensive consideration of the welding torch trajectory and precise control via layered 3D model slicing. This study aims to demonstrate the probability of constructing a complex model using the ABB IRB 1410 in the UTeM Laboratory. The Cura Engine slicing engine was utilized to develop an open-source program called 'Cura' for 3D printing. It can efficiently execute the process of dividing 3D models into layers, determining the path for additive manufacturing, and generating output codes.



## CHAPTER 2

### LITERATURE REVIEW

The research described and analyzed in this chapter were carried out utilizing reference writing materials, such as articles, earlier scientific studies, journals, and reference books. This chapter will discuss about introduction of Additive manufacturing, introduction of Wire Arc Additive Manufacturing (WAAM) and Robotics, path planning and trajectory generation for WAAM Robotic Systems, open-source software for WAAM Robotic System development, welding parameters for WAAM, case studies of WAAM Robotic System development using open-source software and defects and imperfection of welding.

#### 2.1 Introduction of Additive Manufacturing (AM)

3D printing, also known as additive manufacturing, has become a game changing technology with a range of uses across several sectors. It offers benefits like creative freedom, customization and less material waste by enabling the construction of three-dimensional items using layers of materials based on a computer model. A lot of research has been done recently to examine the promise, difficulties and capabilities of additive manufacturing. Rapid prototyping and direct digital manufacture among other additive manufacturing technologies have transformed conventional manufacturing processes claim Edgar and Tint in 2015. They enabled the creation of elaborate shapes and complex geometries that were difficult or impossible to construct using conventional techniques.

The aerospace, automotive, medicinal and consumer products industries have all seen substantial breakthroughs because of this. Wong and Hernandez (2012) highlight the versatility and customizability of additive manufacturing in their review. The fabrication of complex

prototypes, useful components and even entire buildings is now possible thanks to additive manufacturing opening up new opportunities for design innovation. Additionally, improvements in lightweight components and better material utilization have been made thanks to the capacity to construct intricate internal structures and lattices. Additionally, research has concentrated on the creation of novel additive manufacturing processes and materials. Asnafi, (2021) place a strong emphasis on investigating metal additive manufacturing, which uses metals as a feedstock to create functional components with excellent mechanical qualities. As a result, sectors like aerospace, healthcare and automotive have adopted metal additive manufacturing. However, there are certain difficulties with additive manufacturing.

The multi-scale, multi-physics concerns relating to additive manufacturing including temperature management, microstructure control and residual stress mitigation are covered by Qiu & Liu in 2019. For additively made components to be of the highest possible quality, dependability and performance, it is essential to comprehend and address these issues. Another interesting subject is the issues with intellectual property that additive manufacturing raises. In their study published in 2018, Kang et al. explore the problems with patent and design rights protection in additive manufacturing. The ease with which 3D models can be shared and duplicated raises concerns about who owns and controls intellectual property necessitating the creation of the necessary frameworks and rules.

In conclusion, additive manufacturing has transformed manufacturing processes and opened up new possibilities for design, customization, and material utilization. Extensive research has been conducted on various aspects of additive manufacturing, including its applications, materials, processes, challenges and intellectual property concerns. These studies form the foundation for further advancements and utilization of additive manufacturing in diverse industries.

## 2.2 Wire Arc Additive Manufacturing (WAAM) and Robotics

Robotics and Wire Arc Additive Manufacturing (WAAM) are two innovative technologies that have transformed the manufacturing sector. The aerospace, automotive, and medical industries among others, have been significantly impacted by both technologies distinctive benefits. This introduction gives a general overview of WAAM and robotics while emphasizing their significance, uses and possible advantages. Three-dimensional (3D) items are constructed layer by layer using the sophisticated additive manufacturing method known as wire arc additive manufacturing (WAAM). It combines the accuracy and adaptability of robotics with the diversity of arc welding, enabling the cost and time efficient production of complicated geometries and large-scale components. With benefits including lower costs more design freedom and improved structural integrity, WAAM has emerged as a possible replacement for conventional production techniques.

Robotics is an emerging field that has shown great potential for automation and optimization of manufacturing processes, including WAAM. The use of robots in WAAM can significantly improve the accuracy, repeatability and productivity of the process. Robotics can also enable the production of complex geometries that would be difficult or impossible to achieve using traditional manufacturing methods. Due to its combined benefits of greater forming efficiency and lower production costs, wire and arc additive manufacturing (WAAM), a subset of AM technologies, has demonstrated a superior application viewpoint according to Lian (2022). In the 1990s, WAAM first started to take shape and was initially applied to the restoration of metal parts. The procedure has developed through time, and it is now utilized to create substantial metal structures like ship hulls and aviation wings. The use of robotics in production, on the other hand, dates back to the 1960s but recent developments in the field such the development of collaborative robots have increased the scope of its possible uses. The use of robotics in WAAM has several benefits, including increased accuracy, repeatability and

productivity. Robots can also enable the production of complex geometries and reduce the need for skilled labor. However, there are also challenges associated with the use of robotics in WAAM such as the need for specialized programming and integration with the manufacturing process.

There has been a significant increase in the use of open source software (OSS) for various applications. This trend has also impacted the field of robotics and specifically wire arc additive manufacturing (WAAM) robotics. There are several advantages of using OSS for WAAM robotics. One advantage of using OSS for WAAM robotics is that it allows for greater flexibility and customization. The ability to modify and tweak the software code to meet specific requirements or preferences of a particular system is one of the most significant benefits of OSS. Another advantage of using OSS for WAAM robotics is that it can help reduce costs associated with software development and maintenance. ( Xing, 2013) Unlike proprietary software, which requires expensive licenses and regular fees for updates and maintenance, OSS is free to use and can be updated by the community of developers using it. Furthermore, the use of OSS in WAAM robotics can lead to faster innovation and development. This is because developers can share code and build on each other's work, which ultimately leads to faster problem-solving and the introduction of new features. Overall, the use of OSS in WAAM robotics can lead to greater customizability, reduced costs and faster innovation all of which are critical according to Klobčar et al., 2018 in the field of robotics.

Additionally, the open nature of OSS provides transparency and accessibility that is often lacking in proprietary software. This not only promotes collaboration and community building among developers but also allows for greater scrutiny to ensure the software is secure and trustworthy. Another benefit of OSS for WAAM robotics is that it fosters a vibrant and inclusive developer community. This sense of community can help new developers learn from experienced ones, share knowledge and techniques and ensure rapid development. In

conclusion, the use of open source software for WAAM robotics is advantageous in multiple ways. It promotes flexibility, customization, cost reduction, faster innovation and development, transparency and accessibility leading to a vibrant and inclusive developer community. Furthermore, the use of OSS can help democratize access to advanced robotics technologies.

### **2.2.1 Working principle of Wire Arc Additive Manufacturing**

The working principle of Wire Arc Additive Manufacturing (WAAM) involves the deposition of material using an electric arc generated between a consumable electrode wire and the workpiece. WAAM is a layer-by-layer additive manufacturing process that enables the creation of three-dimensional (3D) objects. Several studies have investigated the working principle of WAAM, providing valuable insights into its underlying mechanisms. According to the research conducted by Dong et al. in 2020, the WAAM process begins with the setup and preparation of the workpiece and the robotic system. The workpiece typically made of metal is securely positioned to ensure stability during the deposition process. The robotic system equipped with a welding torch and advanced control mechanisms is programmed to follow a specific tool path. An electric arc is generated between the consumable electrode wire and the workpiece facilitated by a power source that provides the necessary voltage and current.

The work of Prado-Cerqueira et al. (2017) highlights the role of arc characteristics in WAAM. They emphasize the significance of controlling arc length, arc stability, and arc plasma behavior to ensure high quality deposition. The electric arc melts the consumable electrode wire, forming molten droplets of metal. The robotic system precisely controls the movement of the welding torch, positioning it to deposit the molten droplets onto the workpiece surface. Controlling the cooling and solidification rates of the molten droplets is crucial for achieving optimal mechanical properties and structural integrity of the fabricated object. The studies conducted by Su et al. (2019) and Yu et al. (2019) investigate the effect of cooling rates on the microstructure and mechanical properties of WAAM-built components. They emphasize

the importance of understanding heat transfer phenomena and optimizing process parameters to achieve desired material characteristics. Furthermore, the research by Xiong et al. (2020) explores the optimization of deposition parameters in WAAM. They investigate the influence of wire feed rate, arc voltage and travel speed on deposition quality and efficiency. Their findings contribute to enhancing process control and improving the performance of WAAM systems. Figure 2.1 represents the WAAM working principle.

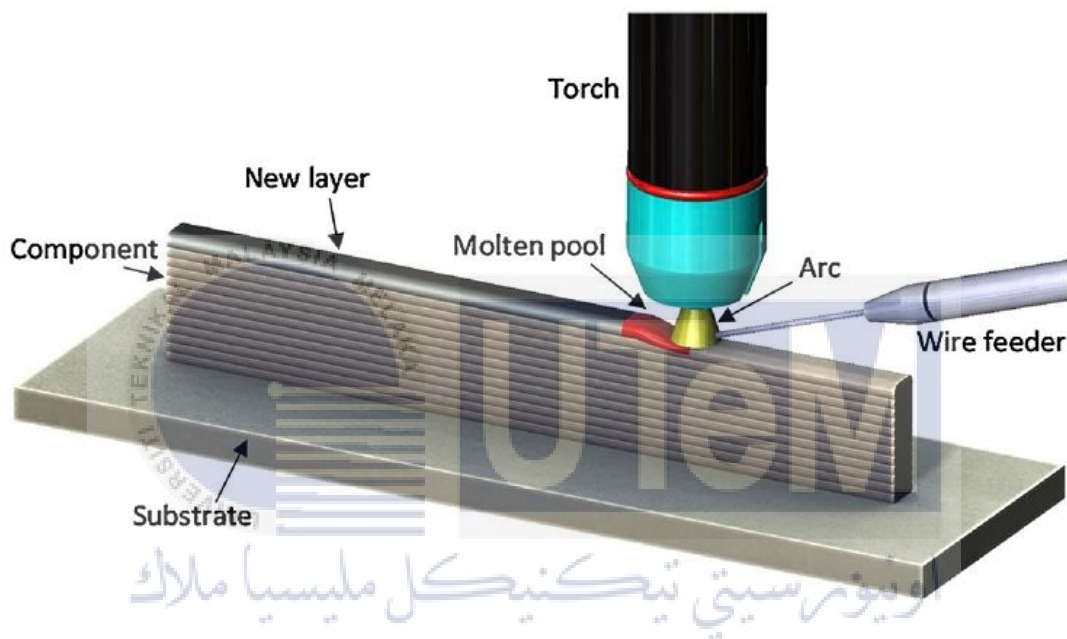


Figure 2.1: Working principle of WAAM, source (Anthony R. McAndrew et al, 2018)

### 2.2.2 Types of principle in Wire Arc Additive Manufacturing (WAAM)

The versatile additive manufacturing method known as wire arc additive manufacturing (WAAM) makes use of automated welding operations to create three-dimensional (3D) items. The purpose of this segment is to examine the many forms and underlying ideas of WAAM. The goal is to learn more about WAAM's many capabilities and prospective uses in the additive manufacturing industry. An in-depth understanding of this manufacturing strategy can be attained by looking at the various WAAM process types and the governing principles that direct their functioning. The categories and guiding principles of WAAM are outlined in this section, illuminating the key ideas that underpin its functionality and potency.

### 2.3 Principle of MIG-WAAM

The fusion-based arc welding procedure known as Gas Metal Arc Welding (GMAW) or Metal Inert Gas (MIG) welding serves as the foundation for Metal Inert Gas Wire Arc Additive Manufacturing (MIG-WAAM). An inert gas barrier and a consumable wire electrode are used in the WAAM variation known as MIG-WAAM to deposit material layer by layer and produce intricate 3D structures. This procedure involves creating an electric arc between the workpiece and the consumable wire electrode, where the heat from the arc melts the wire electrode and creates a pool of molten metal. High quality deposition is ensured by using an inert gas barrier, such as argon or helium, to shelter the molten pool and its surroundings from air pollution. The shielding gas is critical in regulating the arc stability, weld pool form and heat distribution which affects the quality of the finished item in MIG-WAAM, claims a study by Liu et al. (2018).

According to Sameer S. Kulkarni et al., (2019), optimizing process parameters in MIG-WAAM is crucial for achieving the necessary deposition properties. They talk about how welding speed, arc voltage and wire feed rate affect the width, height and shape of the manufactured structures during deposition. In addition, Li et al., (2023) study examines the impact of several variables, including wire diameter, wire extension and shielding gas flow rate on the mechanical characteristics and bead morphology of MIG-WAAM-made components. To guarantee the deposition quality and mechanical integrity of the produced parts, they emphasize the necessity of careful management of these parameters. The research by Gaur et al. (2018) investigates the effects of several wire arc modes, such as pulse, spray, and short-circuiting, on the characteristics and deposition behavior of MIG-WAAM. They go over the benefits and drawbacks of each mode and offer advice on how to pick the one that will best meet the needs of a given application.

Additionally, the modelling and simulation of MIG-WAAM processes are the main topics of Ye et al., (2023). To facilitate process optimization and quality control, they provide mathematical models and numerical simulations to forecast the temperature distribution, thermal history and microstructural evolution during the deposition process.

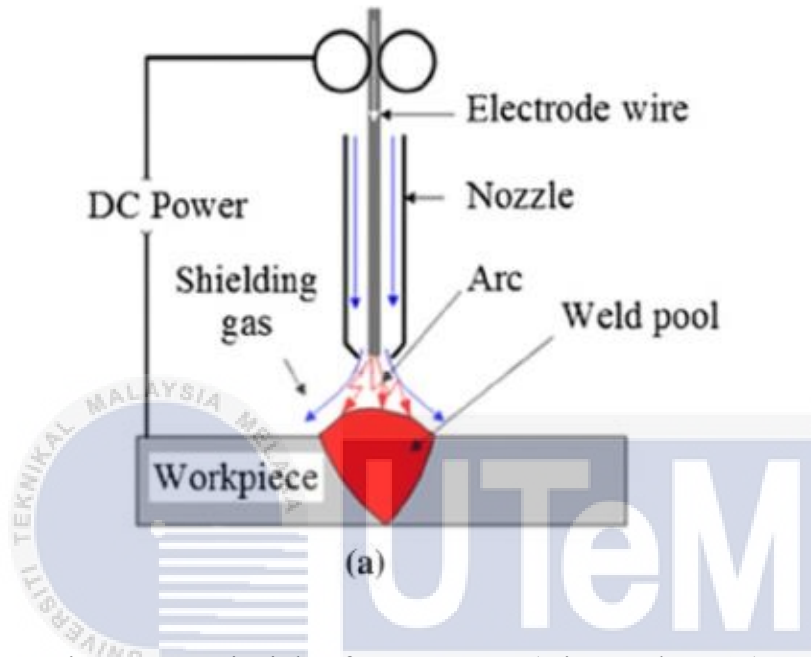


Figure 2.2: Principle of MIG, source (Ding et al., 2015)

## 2.4 Principle of CMT Technology

The regulated metal transfer mechanism at the heart of Cold Metal Transfer (CMT) technology provides considerable benefits for welding procedures. To accomplish regulated droplet transfer during welding, Fronius International's CMT technology makes use of a special wire feeding system and exact control of wire motion, current and voltage. The intermittent retraction and forward feeding of the welding wire which results in a pulsing droplet transfer is the basic idea of CMT technology. The precise transport of tiny droplets from the wire to the weld pool is made possible by the controlled motion of the wire in conjunction with controlled short circuiting.

CMT technique is especially well suited for combining thin or heat-sensitive materials since the pulsing action helps to manage the heat input and lower the total temperature during

the transfer. CMT technology's-controlled metal transport has a few benefits. It first encourages a steady and spatter-free welding process, which improves the quality of the weld. Second, there is less chance of material distortion, deformation, or damage because to the low heat input and low energy usage. Thirdly, improved control over the weld pool is made possible by the controlled droplet transfer producing welds that are accurate and consistent.

Additionally, CMT technology broadens the variety of applications and possibilities by enabling the connecting of incompatible materials with various melting points. The ideas and uses of CMT technology have been the subject of numerous studies, which have shed important light on its capabilities. The influence of process variables, such as wire feed speed and welding current on the droplet transfer behavior in CMT welding for instance are the subject of a study by Lei et al., (2019). They talk about how these parameters affect the properties of droplet dissociation and deposition. Xin et al., (2019) investigate the optimization of CMT welding settings for combining aluminium alloy plates in a separate investigation.

They look at how the mechanical characteristics of the joints and the morphology of the weld beads are affected by wire feed speed, welding current and pulse frequency. Additionally, Madhavan et al., (2016) study investigates the microstructure and mechanical characteristics of dissimilar junctions made of steel and aluminium utilizing CMT technology. They examine the interfacial responses and talk about how welding parameters affect joint quality. The fundamentals of CMT technology, which have been shown by research by Hu et al. (2017), Meng et al. (2019) and Zhang et al., (2013) offer a strong basis for comprehending and applying this sophisticated welding technique.

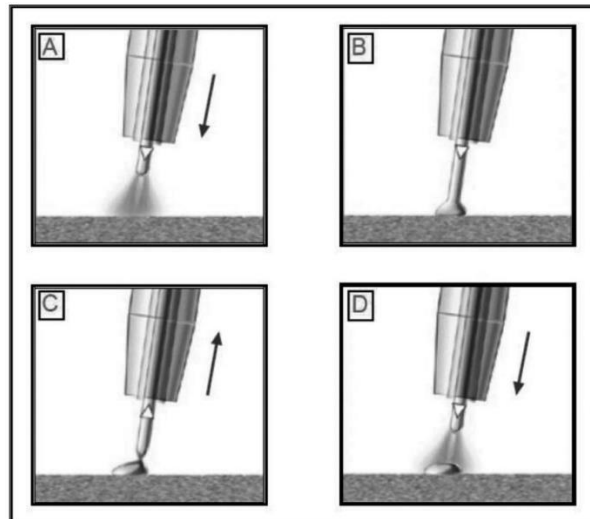


Figure 2.3: A process of CMT method of surfacing by welding, source (Słania et al,2015)

## 2.5 Principle of TIG-WAAM

The Tungsten Inert Gas Wire Arc Additive Manufacturing (TIG-WAAM) technology uses a wire feeding technique in conjunction with a Tungsten Inert Gas (TIG) welding process to deposit material and create three-dimensional (3D) structures. The Wire Arc Additive Manufacturing (WAAM) variation known as TIG-WAAM provides fine control and high-quality deposition. In TIG-WAAM, the TIG welding method is used, in which an arc created by a non-consumable tungsten electrode melts the base metal. A wire electrode is simultaneously supplied into the molten pool adding more material for deposition. The wire feed assures a constant supply of material while the TIG arc generates the heat required to melt the base material and the wire.

The operation and properties of TIG-WAAM have been the subject of numerous investigations. For instance, Feier et al. research (2022) examines how process variables like arc current, wire feed rate, and travel speed affect the deposition quality and mechanical characteristics of components made using TIG-WAAM. They emphasise how crucial it is to optimise these factors in order to get the ideal deposition properties. Furthermore, Murali & Gopi study from 2021 investigates the impact of shielding gas composition on the TIG-WAAM

procedure. They look into how different shielding gases, such as argon and helium, affect the microstructure, deposition quality and dynamics of the weld pool in the produced parts. The study by Ayarkwa et al., (2017) focuses on the wire feeding and arc length control for TIG-WAAM control techniques. They provide control techniques that guarantee constant deposition, precise wire positioning and steady arc characteristics throughout the operation.

Wang et al. work from 2020 also looks on the microstructure and mechanical characteristics of stainless steel components made using TIG-WAAM. They examine how heat input affects the produced parts' grain structure, hardness, and tensile characteristics. Additionally, the study by Schwab et al., (2023) investigates the use of TIG-WAAM in the upkeep and repair of expensive components. They talk about the difficulties and advantages of employing TIG-WAAM for repair applications including as restoring broken parts and boosting their functional efficiency.

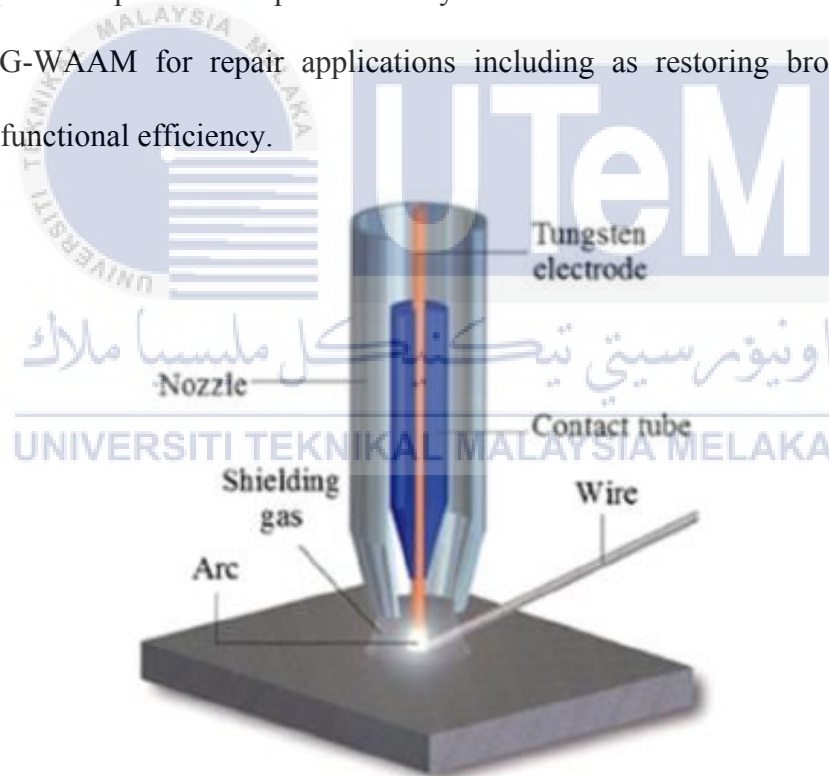


Figure 2.4: Principle of TIG , source (Ding et al., 2015)

## 2.6 Principle of PAW-WAAM

In order to accomplish precise and high-quality additive manufacturing, the Plasma Arc Welding Wire Arc Additive Manufacturing (PAW-WAAM) method integrates Plasma Arc Welding (PAW) with the Wire Arc Additive Manufacturing (WAAM) technique. The

manufacturing of complex 3D structures is made possible by PAW-WAAM, which combines the advantages of plasma arc welding known for its high energy density and fine control with those of WAAM's deposition technology. In PAW-WAAM, a plasma arc is created between the workpiece and a tungsten electrode, creating an intense and highly focused heat source. A wire electrode is simultaneously injected into the plasma arc, where it melts and is then deposited onto the workpiece. The energy needed to melt the wire and the base material is provided by the plasma arc and the wire feed makes sure there is always material available for additive production.

Numerous studies have looked into the fundamentals and traits of PAW-WAAM. For instance, Miao et al. research (2022) examines how process variables such the plasma gas flow rate, wire feed speed, and welding current affect the deposition quality and mechanical characteristics of components made by PAW-WAAM. For the purpose of achieving the necessary deposition properties and mechanical performance, they emphasise the significance of optimising these parameters.

Additionally, Li et al. (2019) research investigates the impact of plasma gas composition on the PAW-WAAM process. They look into how various plasma gases, such argon and helium, affect the plasma arc's properties, the way that materials transfer, and the quality of the deposited material. The control strategies for PAW-WAAM, such as arc voltage regulation, wire feeding control, and motion control of the robotic system, are covered in Chen et al.'s work from 2019. They provide control methods to make sure the additive manufacturing process results in stable arc properties, precise wire positioning, and consistent deposition.

The study by Cheng et al. (2021) further examines the microstructure and mechanical characteristics of titanium alloy parts produced by PAW-WAAM. They examine how different process variables affect the produced parts' grain structure, hardness, and tensile characteristics. Additionally, Zheng et al. (2018) and Dong et al. (2019) investigated the use of PAW-WAAM

in various materials and industries. The mechanical parameters of aluminium alloy components made using PAW-WAAM are studied by Zheng et al. (2018). Dong et al. (2019) highlight the opportunities and problems associated with fabricating large-scale structures utilising PAW-WAAM.

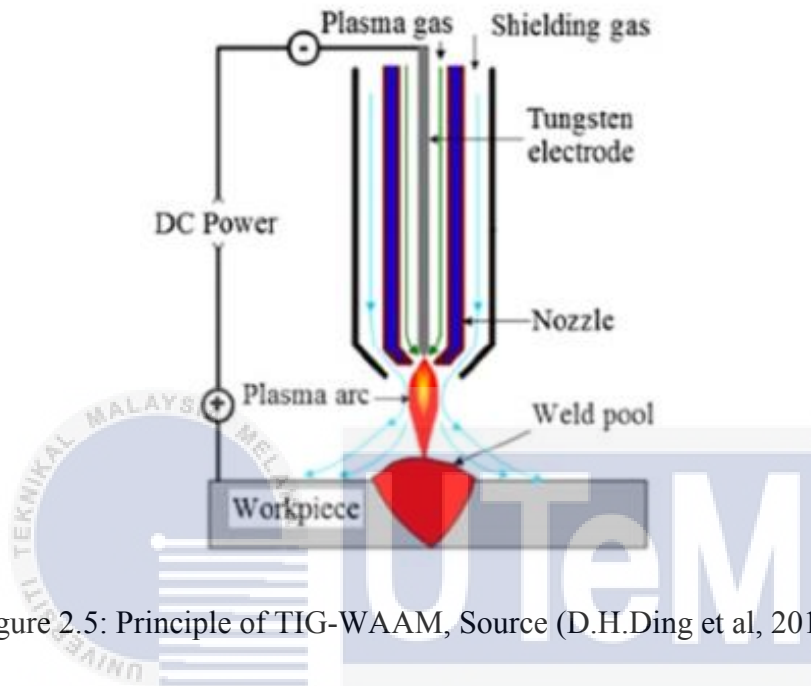


Figure 2.5: Principle of TIG-WAAM, Source (D.H.Ding et al, 2015)

## 2.7 Robotic motion mechanism

Robotic motion mechanisms are essential parts of robotic systems that give robots the ability to move and carry out activities in a precise and controlled way. Robots may explore their environment, interact with objects, and complete certain tasks using these systems, which are created to mimic or reproduce human-like actions. Robotic systems may perform a variety of actions, including translation, rotation, articulation, grasping, and more, by combining mechanical parts including joints, linkages, actuators and sensors. Robotic motion mechanisms must be carefully planned and implemented if the robot is to be agile, dexterous and capable of carrying out complicated tasks in a variety of settings, including manufacturing, healthcare, exploration and other fields. In the previous research, there are some types of motion of robot

mechanism such as six joint robotic mechanism, three dimensional printing mechanism and CNC robotic motion mechanism.

## 2.8 Six joint axes robotic mechanism

According to R. Aparnathi and V. V. Dwivedi (2014), 6 DOF robotic arms are the type of robots employed in the majority of industries because they can accurately position and rotate their end effectors. Over past few decades, a variety of methods have been studied to give robotic arms six degrees of freedom for motion, with the most popular ones being those with rotating joints and wrists with intersecting axes. Currently, these robots and their typical mechanisms of motion are used in the majority of businesses. Due to the robot's wrist's intersecting axes, a rectifier mechanism must be positioned in arm 3 in order to set up the entrance rotational axes for joints 4, 5 and 6. In order to give a robotic arm six degrees of freedom of motion, Mohsen Shahhosseini (2014) describes their effective mechanism design and kinematic modelling. This allowed them to efficiently control the motion of the robotic arm. Parallel principles underlie this system's operation, according to C. Hoberman (2013). They specifically adapted certain 4-bar linkage systems and combined them in parallel to create this mechanism. By doing this, they were able to transfer the rotational motion of the joints 3, 4, 5, and 6 motors to the rectifier mechanism for the other joints and to joint 3's main rotational axis. Figure 2.6 shows the six axis of robotic arm that used in industrial automotive.

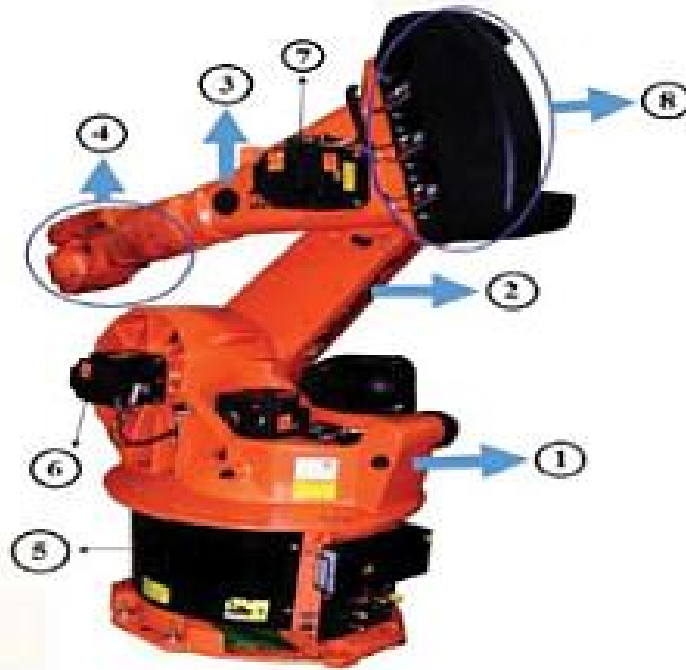


Figure 2.6: Six axis of robotic arm, source (Rambod Rastegari, 2016)

## 2.9 3D printing robotic mechanism

In order to meet the growing demand for customization and three-dimensionality at an affordable price, other manufacturing technologies have evolved in the sensors sector in recent years (Y. Xu, 2017). It is true that conventional microfabrication techniques, such as surface or bulk micromachining procedures, which are restricted to 2D (Choi J-W, 2009) or 2.5D (Corigliano A, 2007) structures, cannot produce fully 3D structures for electro-mechanical sensors. There are several instances of 3D printing processes that enable the integration of mechanical sensors and their electronics into a single printed object in the literature (D. Espalin, 2014). The capacity to move along three separate axes is a fundamental component of motion used by nearly all 3D printers, laser cutters, and CNC routers. This same idea underpins 2D movement in 3D printing. On a 3D printer, the X axis typically signifies lateral movement from left to right (or vice versa), and the Y axis denotes forward and backward movement. It's crucial to understand that a 3D printer's X and Y axes can only depict 2D motion. However, the Z

axis gives 3D printers a third dimension. A 3D printer can move up and down in addition to its 2D movement, unlike a regular printer or pen.

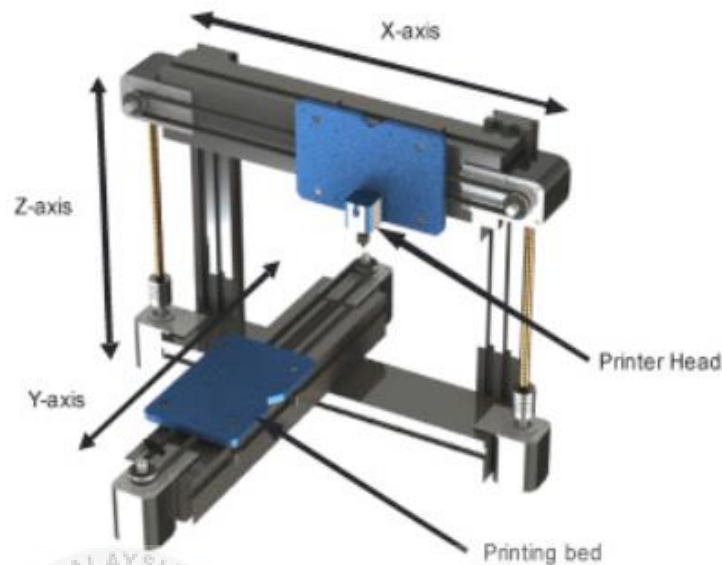


Figure 2.7: 3D printing with X, Y and Z axis label, source (A.Munaz et al, 2016)

## 2.10 Material description and Welding Consumable

(Anna Ermakova, 2020) claims that WAAM (Wire and Arc Additive Manufacturing) technology is employed in many industries and is effective for producing large-scale goods. Using (Haden, 2017) as a reference, researchers looked at the mechanical characteristics of WAAM mild steel specimens and discovered that the composition of printed steel specimens is the same as that of wrought steel. Similar yield strength values were found for the uniaxial tensile strength of wrought low carbon steels and samples of WAAM mild steel. The material characteristics of steel structures, such as Young's modulus, yield and tensile strengths, ductility and fatigue resistances have a significant impact on how well they perform structurally. Sian I. Evans et al (2022) state for traditionally manufactured steel structures, these material qualities have been thoroughly investigated leading to the establishment of standardised production processes and the creation of associated design guidelines. These material characteristics are highly variable for WAAM components since no standard WAAM

manufacturing parameters have been established for structural applications. When a result, this part reviews the essential material characteristics of WAAM steel structures and explores how they change when manufacturing parameters change. A list of tensile material test of stainless steel and carbon steel made by WAAM had been executed into the Table 1 with information on material grade, angle of extraction, printing parameter used and post processing method employed.

Table 1: List of tensile test material Stainless steel and carbon steel, Source (S.I. Evans et al, 2022)

Steel grade	No. of tests	Angle (°) of extraction	Details
308LSi (P. Kyvelou et al,2020)	12M, 39AB	0,45,90	WFS 4-8m/min
304L (L. Ji,2017)	6M	0, 90	WFS 1 m/min only average results reported.
304L (V. Laghi, 2020)	9M	0, 45, 90	Active cooling used, WFS 4–8 m/min.
308LSi (C. Buchanan et al, 2018)	6M	0, 45, 90	Initial voids detected.
ER70S-6 (I. Tarus, 2021)	8M, 14AB	0, 45, 90	Only average results reported.
308LSi (V. Laghi, 2022)	2M, 8AB	0, 45, 90	WFS 0.6-2m/min.
308LSi (V. Laghi, 2018)	2M, 9AB	0, 90	Porosity detected
ER70S-6 (H. Xin, 2021)	8M	0, 45, 90	MIG
308L (V.T. Le, 2021)	6M	0, 90	MIG with variable WFS, 40s dwell time.
304L (J.V. Gordon, 2018)	7M	0, 90	Average results reported only.
316LSi (C.R. Cunningham, 2019)	24M	0,90	WFS 2 m/min, only different combinations of heat input and interpass

			temperature used, average results reported.
308LSi (V. Laghi, 2021)	12M, 32 AB	0, 90	WFS 4–8 m/min, active and uncontrolled cooling used, only graphical results reported.
316L (C.R. Cunningham, 2021)	6M	0, 90	WFS 2 m/min, only in process cryogenic cooling compared to interpass temperature control, graphical results reported.
304 (C.V. Haden,2017)	8M	0	WFS 5.4 m/min, only graphical results reported.
ER70S (C.V. Haden,2017)	7M	0, 90	WFS 2 m/min, only in process cryogenic cooling compared to interpass temperature control, graphical results reported.
316L & 316LSi (C.R. Cunningham, 2020)	>100M	0, 90	Combinations of different heat inputs, cooling strategies and deposition rate used. Only graphical results reported.
ER70S-6 (E. Aldalur, 2020)	24M	0, 90	WFS 8 m/min. Different path planning strategies used. Only average results reported.
ER70S-6 (V.T. Le, 2020)	6M	0,90	Dwell period of 60 s.
ER70S-6 (A. Ermakova, 2020)	4M	0,90	Average result period only.
ER100S-1 (A. Ermakova,2020)	4M	0, 90	Only average result period.

M- machined

AB- as built

Two varieties of stainless steel welding wires that are appropriate for low temperature welding were picked for the current study. In the ER70S-6, deoxidizers are utilised to enhance material yielding, welding travel speed, and wetting, all of which boost productivity and extend consumable life. This material is a great option for marine applications because it is perfect for welding mildly blemished steels. The Cold Metal Transfer (CMT) based WAAM technique was employed in conjunction with the display of manufacturing parameters. The basis plates for the study were selected using EN10025 rolled structural steel with dimensions of 420 x 200 x 12 mm. Clearly demonstrate how the discovery was made. The ER70S-6 specimens used in this study have hardness values between 137 and 180 High Voltage, yield stresses between 365 and 390 MPa, and Ultimate Tensile Strength values between 518 and 522 MPa. This investigation's average fracture toughness value for ER70S-6 is 420.11 kJ/m<sup>2</sup>, which is a little bit less than the figure listed in the literature.

According to the journal (Tomer Ron, 2019), both the corresponding wrought steel alloy (ST-37) and the WAAM steel samples (ER70S-6) are low carbon steels with remarkably similar chemical compositions. The welding procedure was carried out using a welding manipulator, which was composed of a welding robot and a numerically controlled computer.

According to the hypothesis published in the journal (SLM), powder bed technologies like electron beam melting (EBM) and selective laser melting are the main focus of current additive manufacturing (AM) processes. But these processes have a number of disadvantages, including high energy consumption, pricey metal powder, and component size restrictions brought on by the size of the printing cell. The technique was discovered to be current additive manufacturing. The findings demonstrated that both alloys had adequate stress corrosion resistance and that the general corrosion resistance of the wire arc additive manufacturing WAAM samples was comparable to that of the matching ST-37 steel. The following goals

guided the fatigue crack growth testing on compact stress specimens taken from ER70S-6 steel WAAM produced components.

(Mehmanparast, 2021) states that the fracture propagation behaviour of specimens removed with varied orientations (i.e., horizontal and vertical with respect to the deposition direction) was investigated under two different cyclic load levels. The study's findings regarding fatigue growth trends and Paris law constants help design guidelines for unique functionally graded structures created using WAAM technology. This project required the usage of ER70S-6 copper-coated carbon steel welding wire. The cutting edge additive manufacturing technique known as wire and arc additive manufacturing (WAAM) has the ability to improve the design and efficiency of structural component materials while also bringing down production costs. As a result of the layer's recurrent and periodic melting, solidification and warming the WAAM deposition technique results in some elastic, plastic and viscous deformations in additively constructed components. Table 2 shown the composition of materials used for ER70S-6 and ER100S-1 wire with 10 materials used (wt.-%).

Table 2: Chemical Composition of material (wt.-%), Source (A.Ermakova et al, 2020)

Element	C	Mn	Cr	Si	Ni	Mo	S	P	Cu	V
ER70S-6	0.09	<1.60	0.05	0.09	0.05	0.05	0.007	0.007	0.20	0.05
ER100S-1	0.08	1.70	0.20	0.60	1.50	0.50	-	-	-	-

### 2.11 Open-source software for WAAM

The effectiveness of WAAM can be improved by utilising a variety of open-source software choices. For instance, “FreeCAD” a free and open-source 3D modelling programme with parametric features, offers a flexible framework for building intricate shapes in WAAM procedures (Bradford et al., 2020). In addition, creating high-quality meshes for WAAM

simulations frequently uses Gmsh, an open-source finite element meshing programme (Geuzaine & Remacle, 2009). Customised designs and parametric models can be created in WAAM applications using “OpenSCAD”, an open-source script-based CAD programme (Müller, 2013). An open-source programme called “PyCAM” could produce toolpaths and G-code for WAAM processes, which makes process planning and optimization easier (van Vliet, 2015). “Slic3r”, which enables the creation of optimized toolpaths and the slicing of 3D models for additive manufacturing, is another useful piece of open-source software for WAAM (Pra, 2011). Additionally, “MeshLab”, an open-source mesh processing programme, provides mesh editing, repair, and analysis functions that can be helpful for WAAM post-processing and quality control (Cignoni et al., 2008). “OpenFOAM”, an open-source computational fluid dynamics (CFD) programme offers a stable foundation for modelling heat transfer and fluid flow for the simulation and study of WAAM processes (Weller et al., 1998). Real-time data collecting and analysis can be made possible in the context of process monitoring and control by using open-source hardware platforms like “Arduino” (Banzi, 2011) and “Raspberry Pi” (Upton & Halfacree, 2012). Additionally, the incorporation of open-source machine learning frameworks like “TensorFlow” (Abadi et al., 2016) and “scikit-learn” (Pedregosa et al., 2011) can improve the predictive capacities and quality control in WAAM processes.

The previously listed software programmes, such as “FreeCAD”, “OpenSCAD”, “PyCAM”, “Slic3r”, “TensorFlow”, “scikit-learn” and “MeshLab” provide easily accessible platforms for design, process planning, optimization, quality control and mesh processing in applications involving wire arc additive manufacturing (WAAM). Users of these open-source tools can progress and better comprehend WAAM, encouraging creativity in the additive manufacturing industry. These software alternatives allow for the acquisition of important insights that result in improved designs, optimized procedures, and increased quality control in WAAM. Open-source software makes it possible for academics and students to actively

contribute to the creation and study of WAAM technologies, fostering innovation and advancement in additive manufacturing.

## 2.12 Welding Parameter

The method parameters used have a significant impact on the quality of the welded connection (Srivastava, 2010). The welding input parameters have a significant role in determining the quality of a weld connection. Weld-bead shape, mechanical properties, and distortion can all be used to assess the quality of a junction. All welding techniques are often used to create welded junctions with the appropriate weld-bead characteristics, good mechanical qualities, and little distortion. The impact of welding settings on WAAM procedures has been thoroughly investigated by researchers. For instance, Li et al. (2019) investigated how arc current and voltage affected the mechanical characteristics, microstructure, and deposition rate of WAAM parts. They discovered that raising the arc current and voltage enhanced the velocity of deposition while also adding more heat to the process, which had an impact on the microstructure and mechanical characteristics of the material being deposited. Wang et al. (2020) conducted a study to investigate the effects of wire feed rate and travel speed on the geometry, microstructure and mechanical characteristics of parts produced by WAAM. They noticed that while faster travel speeds caused bead height and width to decrease, faster wire feed rates caused bead width to increase.

Another important factor in WAAM is the composition of the shielding gas. Kim et al. (2018) looked at how the composition of shielding gas affected the porosity, microstructure, and mechanical characteristics of stainless-steel parts produced by WAAM. They showed that compared to pure argon, using a mixture of argon and helium as the shielding gas resulted in less porosity and better mechanical qualities. Researchers have also looked into how various welding factors interact with one another. In 2020, Xu et al. investigated the combined impact of arc voltage and travel speed on the microstructure, residual stresses and bead shape in

WAAM-built products. They discovered that greater bead width and decreased residual strains were produced by raising arc voltage and lowering travel speed. The influence of other welding parameters on WAAM processes such as wire diameter and nozzle-to-substrate distance has also been studied in several research investigations (Tang et al., 2021; Wang et al., 2021).

Finding suitable welding parameters for welding voltage, welding current and welding speed, as well as looking into how welding parameters impact the joining process are the main objectives of this study. Low carbon content is used in the material. The filler is made of steel A1008 and AWS ER 70S-6. Many industries, especially the automotive sector, currently use robotic welding technology for the joining process, according to (N.D. Pandey, 195-211). In comparison to the conventional human welding approach, the robotic welding process has several benefits, including better weld quality, a quicker turnaround time, less waste and reduced costs. Although robot welding is very popular, welding parameter modification must be done by hand. For the robot to be precise and for the welding of the butt joint to be of high quality, precise specifications are essential.

A few trial runs were carried out on IS 2062 mild steel plate (6 mm thick), according to S. Srivastava and R.K. Garg (2020), to determine the practical and effective working limitations of the gas metal arc welding parameters included in this study under the conditions listed in figure 2.8. The trial runs have been conducted using various configurations of MIG process parameters. The functioning parameters of the chosen parameters have been determined by visual examination and bead geometrical appearance. Porosity and overlap at the weld edges were seen at voltages lower than 24 V. On the other hand, porosity, splatter and undercut are seen at voltages higher than 32 V. Blowing holes and porosity are the main defects that are seen when the shielding gas flow rate is less than 10 lpm. However, gas entrapment was noted when the gas flow rate exceeded 18 lpm. Shallower penetration, a broader weld bead, and overlap were noted for travel speeds under 160 mm/min. On the other hand, fusion

is incomplete and the rate of material deposition is poor for transit speeds more than 220 mm/min. Badly formed weld beads and spatters were seen when the wire feed rate was higher than 9.5 m/min, whereas partial fusion flaws and reduced penetration were seen when the wire feed rate was lower than 4.5 m/min.

Polarity	DCRP (Electrode Positive)
Welding Current	150–250A
Electrode	Copper Coated Mild Steel Wire
Electrode Diameter	1.2mm
Shielding Gas	CO <sub>2</sub>
Torch Position	Inclined
Operation	Automatic

Figure 2.8: Welding condition, source (S. Srivastava,2020)

For dissimilar joint metals, previous writers have used the shielded metal arc welding (SMAW) technique. Manikandan et al. (2017) used SMAW to combine the stainless steel AISI 316L and the nickel-based superalloy Incoloy 800 with a welding current of 150 A and an arc voltage of 13 to 15 V. The welding settings used by Verma et al. (2016) to successfully combine 316L ASS and 22% Cr DSS 2205 were 70-120 A and 16-25 V for the current and arc voltage, respectively. Verma et al. (2016) conducted a further investigation in which they joined A2205 and SS316L using a welding current of 120 A, a welding speed of 3.1–3.3 mm/s and an arc voltage in the region of 25–26 V. Due to the numerous, both controllable and uncontrollable components involved in the welding process, optimizing dissimilar welding becomes difficult. Through the Taguchi method, Ghosh et al. (2017) reported the impact of welding parameters GMAW on the mechanical characteristics of AISI 409 and AISI 316L. Daniyan et al. (2018) used the Taguchi approach and response surface methodology (RSM) to analyze welding

parameters and produce predicted weld distortion and hardness models. In order to examine how welding parameters affect steel's hardness and flexural strength and to get the optimal values, Mahmood and Alwan (2019) also used the Taguchi method technique.

As shown in Table 3, four welding parameters were chosen: electrode type, welding current, arc voltage, and welding speed, according to Diah Kusuma Pratiwi (2023). The parameters were chosen using equipment settings and welding technique parameters that are generally accepted. A 2.6 mm diameter, two-layer electrode was used for welding. The orthogonal array (L9)'s experimental design and factor distribution are also displayed in Table 4.

Table 3: Factors and level for the welding process, source (Diah Kusuma Pratiwi ,2023)

Parameters	Level 1	Level 2	Level 3
Electrode type (A)	E308	E309	E312
Welding current (B)	90	100	110
Arc voltage (C)	14	16	18
Welding speed (D)	4	5	6

UNIVERSITI TEKNIKAL MALAYSIA MELAKA

Table 4: Experimental layout and factor distribution of the orthogonal array (L9), source (Diah Kusuma Pratiwi ,2023)

ExpNo	Factor				Experimental welding values			
	A	B	C	D	Electrode	Current (A)	Voltage (V)	Speed (cm/min)
1	1	1	1	1	E 308	90	14	4
2	1	2	2	2	E 308	100	16	5
3	1	3	3	3	E 308	110	18	6
4	2	1	2	3	E 309	90	16	6
5	2	2	3	1	E 309	100	18	4
6	2	3	1	2	E 309	110	14	5
7	3	1	3	2	E 312	90	18	5
8	3	2	1	3	E 312	100	14	6
9	3	3	2	1	E 312	110	16	4

### 2.13 Cooling rate

It is increasingly popular to use WAAM (wire and arc additive manufacturing) to create components from metals that are frequently unsuitable for traditional production processes. An excellent example is duplex stainless steel (DSS) which is challenging to weld and process. However, if the interlayer temperature is too low, the process would take longer overall and the high productivity of WAAM will be compromised. In order to determine the correlation between interlayer temperature and process duration, different interlayer temperatures (50 °C, 100 °C and 150 °C) were investigated. Surface texture, chemical composition, ferrite content, porosity appearance and hardness were all analyzed. Rahul Sharma (2020), say that in addition to the metallurgical consequences, the interpass temperature also affects the component's danger of thermal overheating and the size of the molten pool. This is why it is advantageous

to wait until the component has cooled to a specific temperature before continuing with the welding. There were no appreciable variations in the samples' surface texture or chemical composition but lower interlayer temperatures led to more ferrite and higher porosity. Interpass temperatures typically range from 50 °C to 120 °C depending on the materials being treated and the experimental setup.

Various research groups conducted investigations on how interpass temperature affects the component qualities. Da Silva et al. (2018) conducted the initial studies with cooling techniques for WAAM. Here, uncooled welds and water bath cooling procedures were used to compare their impacts. The entire component was kept in a canister that contained water. To maintain a constant distance from the weld bead, the water level was gradually raised along with the welding layers. The experiments revealed that the water bath cooling appears to be extremely effective for quickly lowering the workpiece temperature after welding. Other cooling solutions, however, might be of interest given that the water bath is problematic, particularly in multi-axis manufacturing systems with moving worktables. Li et al. (2019) looked at a comparable method of cooling the component side walls using a totally different cooling technique. In order to create an active cooling effect, Peltier components were mounted to the sides of wall-shaped constructions as a cooling mechanism. To maintain a steady thermal condition and provide a satisfactory contacting surface for the Peltier components, single weldments were deposited on upward-positioned plates to evaluate the cooling strategy. However, it could be challenging to apply the method to geometrically more demanding components.

Hackenhaar et al. (2019) carried out more research employing an air jet cooling system. Here, a high-pressure air jet was used to cool the workpiece before, during, and after the welding process. The air jet was directed at the lower side of the created wall-shaped structures rather than directly at the welding zone to prevent disruption of the operation. The findings

demonstrate that it was possible to significantly shorten the interpass cooling period. Wu et al. (2018) conducted comparable research utilizing a CO<sub>2</sub> jet rather than a high-pressure air jet. Effective cooling techniques are crucial for the implementation of a successful WAAM-based process chain, considering the effects of cooling rates on mechanical and geometrical qualities as well as on production speed.

The cooling techniques that have been researched up to this point are either incapable of in situ cooling during the welding process or very effective in terms of cooling performance but difficult to handle for fabricating complicated components. An effective, highly adjustable, adaptable, and affordable cooling method may be found in the aerosol cooling strategy.

#### **2.14 Welding Imperfection and defects**

A poorly trained or inexperienced welder's technique or structural issues during the welding process might result in welding defects. Even though the mechanical characteristics of parts made using WAAM are frequently on par with those of their traditionally processed equivalents, several processing flaws in AM must be fixed for applications that are crucial. For parts exposed to extreme environments where these faults contribute to failure modes such as excessive heat, porosity, overlap, lack of fusion must be avoided. According to B. Wu et al. (2017), thermal deformation associated with heat accumulation, unstable weld pool dynamics due to poor parameter setup, poor programming strategy, environmental influence (such as gas contamination) and other machine malfunctions can all lead to defects in WAAM. In contrast, during the welding process, the size and shape of the metal structure change. It might be caused by the employment of an inappropriate welding approach or by the wrong welding process. The filler metal and edge preparation must fuse together sufficiently for a perfect or satisfactory weld.

### 2.14.1 Excessive heat

When the parent metal being welded to warps because of the welding process's extreme heat, distortion may develop. Due to their lack of surface area for heat dissipation, thinner gauge sheet metals typically experience this. Due to the metal being exposed to heat for a prolonged period when making lengthier welds, it can also happen in certain situations. Stress distortion is seen when a material's internal residual stress exceeds its yield. It results from the metal's unequal expansion and contraction. According to D. Boothy (2014), there are two ways to classify welding distortion: in-plane welding distortion and out-of-plane welding distortion. After welding, distortion alters the shape of the component, and the way it happens. Again, the three types of in-plane welding distortion are angular, transverse, and longitudinal distortion. A particular kind of out of plane welding distortion is buckling distortion. Figure 2.9 shows the classification of distortion.

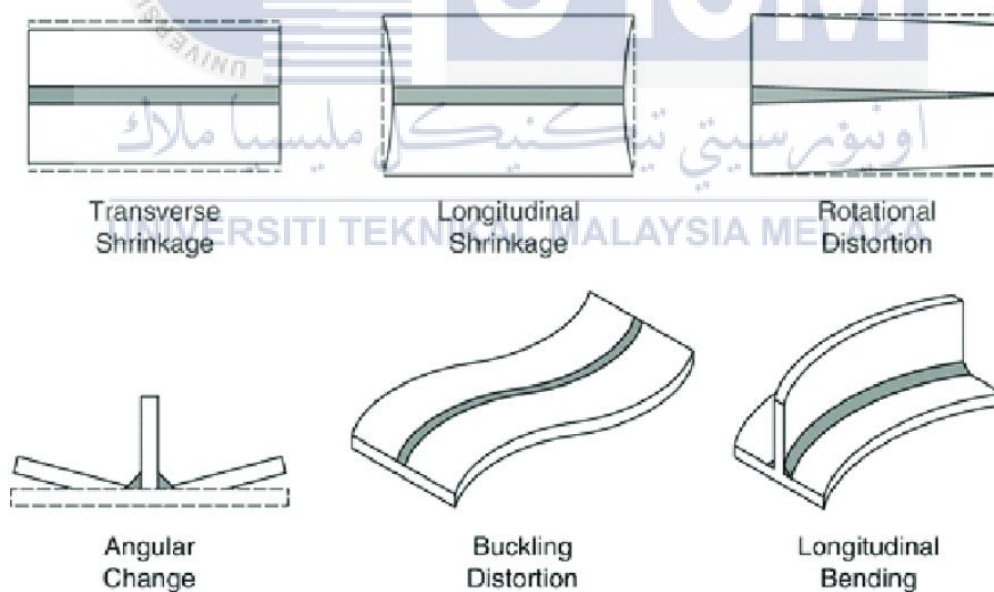


Figure 2.9: Classification of distortion, source (Zuheir Barsoum,2015)

### 2.14.2 Porosity/ Gas bubble

A typical welding flaw known as porosity is defined by the presence of gas bubbles or voids inside the weld metal. The integrity and mechanical characteristics of the weld joint may be considerably impacted. Numerous elements, such as the welding method, welding parameters, base metal composition, and shielding gas employed, have an impact on porosity creation. Porosity is mostly caused by gas entrainment during the welding process. Gases like hydrogen, oxygen, or nitrogen may get caught in the metal during the welding process. The development and prevention of porosity in austenitic stainless steel weld metal are highlighted by Lippold et al.'s 2000 study. The study sheds light on the processes and variables that contribute to the establishment of porosity. Porosity can also be caused by contaminants on the surface of the base metal. When heated by the welding arc to its high temperatures, oil, grease, moisture or dirt can release gases. To reduce the creation of porosity, the base metal surface must be cleaned properly (Kou, 2003).

Porosity during welding may come from inadequate shielding. The weld pool may absorb ambient gases due to inadequate shielding gas covering or insufficient gas flow. In their 2011 study, Dias et al. used image processing and X-ray radiography to assess the porosity in welded connections. Characterization and analysis of porosity faults are the main topics of the study. To reduce porosity, welding parameters must be optimized. Overheating can increase the possibility of porosity and lead to excessive base metal vaporization. To prevent the creation of porosity, Naidu (2011) emphasizes the significance of controlled heat input and good welding process. Strategies for preventing and reducing porosity include appropriate cleaning, sufficient shielding, controlled heat input, and appropriate welding technique. Shah and Panda (2012) examine how porosity develops during the laser beam welding of aluminium alloys, illuminating the factors that affect porosity and outlining strategies for reducing it. Figure 2.10 shows the porosity while running experiment based on the T. Hauser et al., in 2021.

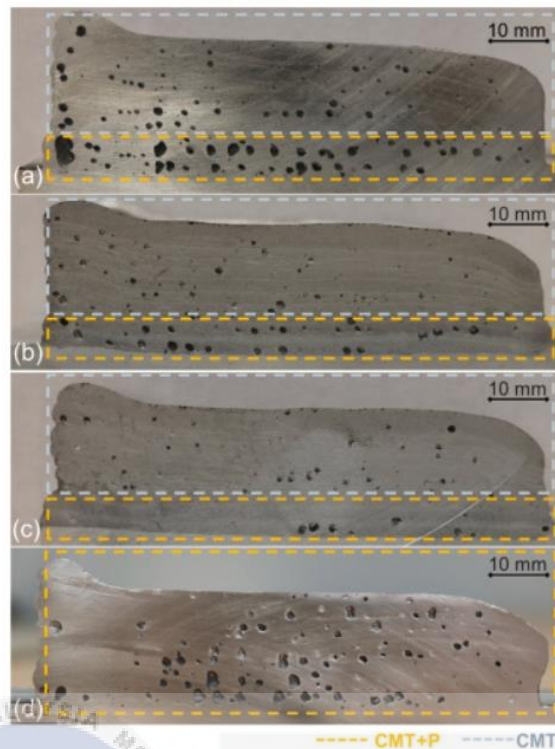


Figure 2.10: Porosity while running experiment, source (T. Hauser et al., 2021)

### 2.14.3 Overlap

The bulge of welded metal above the root is known as overlap welding. A protrusion that extends past the weld toe called the overlap. Even while overlap is more of a weld discontinuity than a defect, it is nonetheless categorized as one. Overlap typically happens in butt and fillet welds. The presence of an overlap indicates that the metal has not bonded entirely. An overlap typically looks like a circle that is larger than necessary. They are more prone to happen when hand arc welding is being done since the weld integrity depends greatly on the competence and health of the welder on any given day. The welder cannot clearly see the movement of the welding rod due to the intense light produced during welding, which has an impact on the welding quality based on the welder's expertise. According to (Liu, G, 2022) undercut and overlap flaws of the weld bead can also result from poor welding electrode movement. According to B. Shushma et al. in 2019, this fault appears when the weld face extends past the weld toe. The weld metal rolls in this situation, forming an angle that is less than 90 degrees.

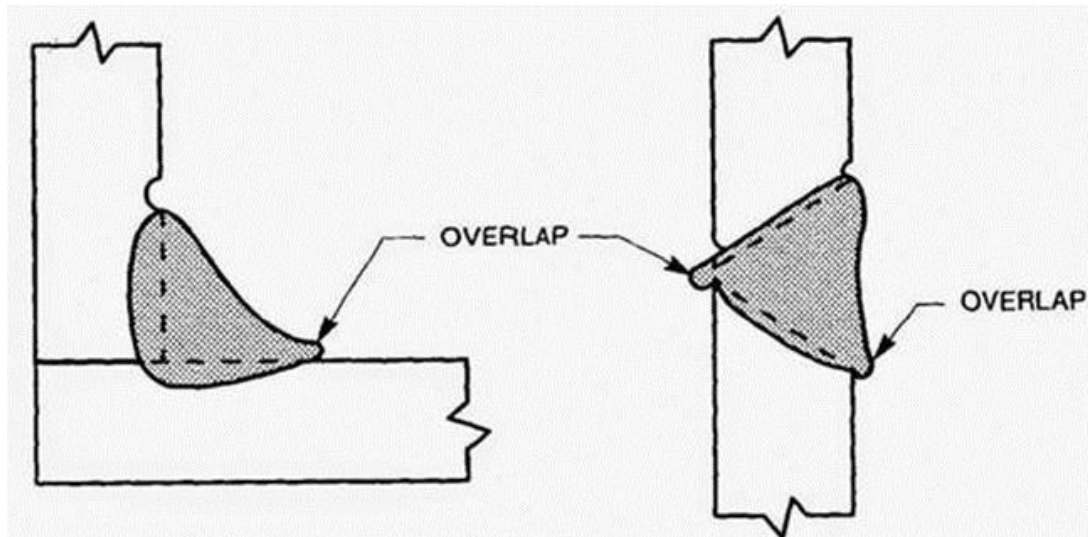


Figure 2.11: The schematic of overlap, source (Blockadvtech, 2018)

#### 2.14.4 Lack of fusion

When the parent metal and the weld metal do not fully attach to one another, this happens. When a weld does not start at the weld groove's root, there is a lack of penetration. These typically happen because of subpar welding skill, most likely a wrong angle, too much speed, or an inadequate arc length. This may result in a weak or transient connection. According to Janez Grum (2008), lack of fusion, a planar defect that is challenging to find using standard NDT techniques, can have disastrous results because it endangers not only the integrity of the pressure vessel but also the environment and the health of the workforce. Ren M. et al. (2012) claim One of the most critical edge weld flaws, lack of fusion, can frequently happen during the welding process, severely destroying joint quality and leading to seal failure. Although the fabrication process is closely monitored and controlled, occasionally there is a lack of fusion when MPAW is used to manufacture ultra-thin-walled components such as the aircraft accumulator bellows.

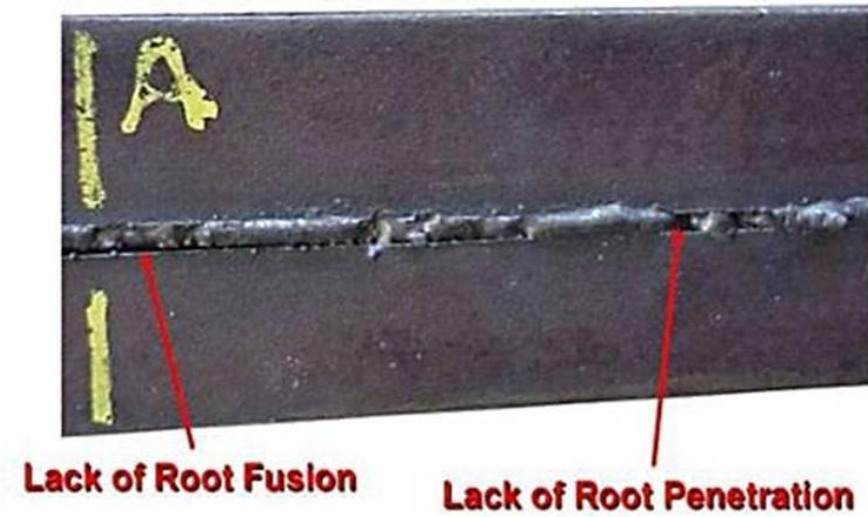


Figure 2.12: Schematic of lack of fusion, source (Blockadvtech, 2018)



## CHAPTER 3

### METHODOLOGY

#### 3.1 Introduction

This chapter will explain the method and procedure for performing the path planning method, a three-dimensional model structure using robotic based on wire arc additive manufacturing and analyze the geometrical characteristic of three-dimensional structure. The parameters varied in this study to weld the model structure. This chapter will include the process from the beginning of the research until the 3D model structure weld.

#### 3.2 Gantt Chart

As shown in Appendix A.



### 3.3 Progress flowchart

Figure 3.1 illustrates the progress flow from the start on the project until the end of the project.

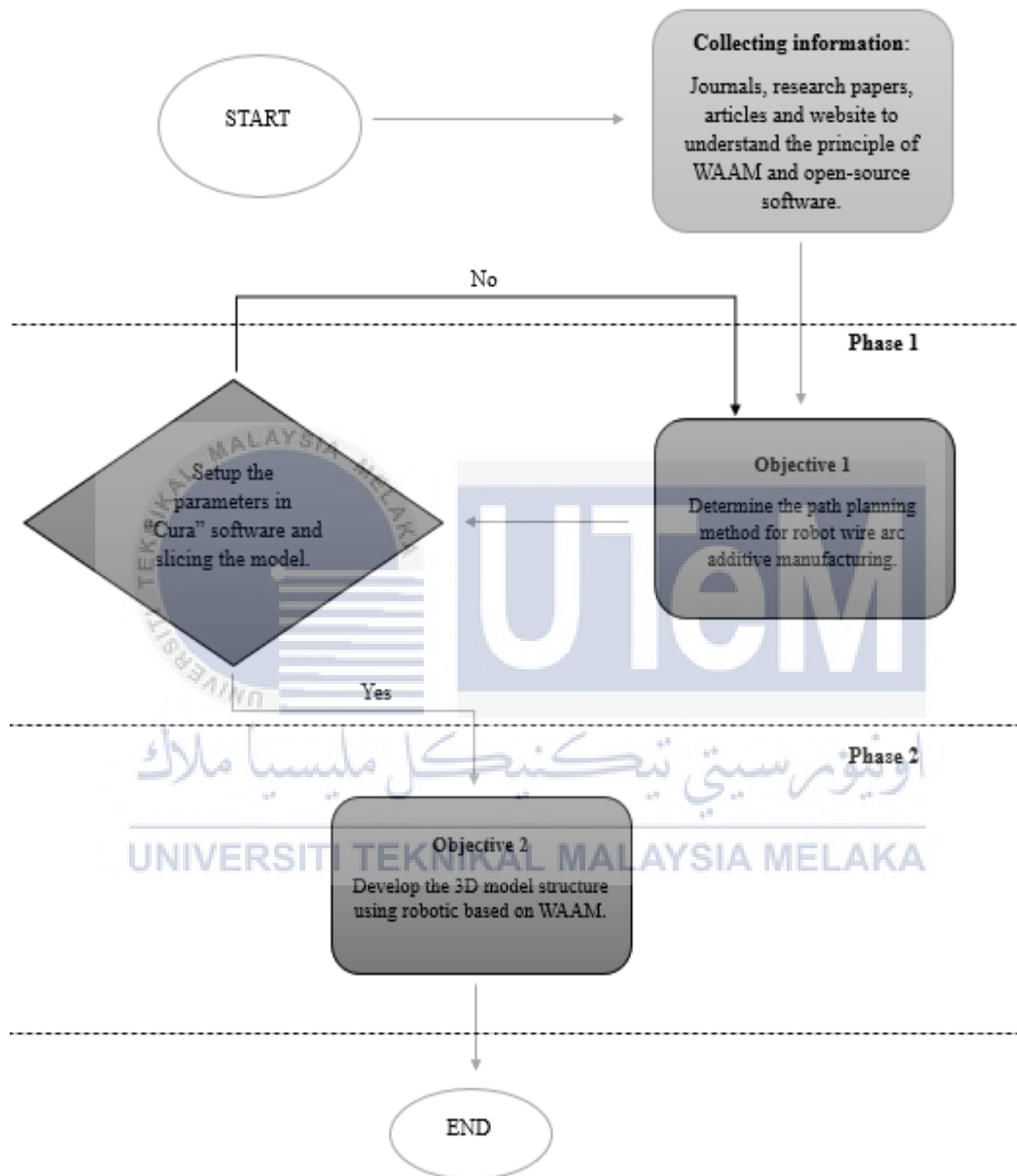


Figure 3.1: Research flow Chart

### 3.4 Wire arc additive manufacturing process

Figure 3.2 represents the wire arc additive manufacturing process in this study from the start until the robot welding finishes to weld the three-dimensional model structure.

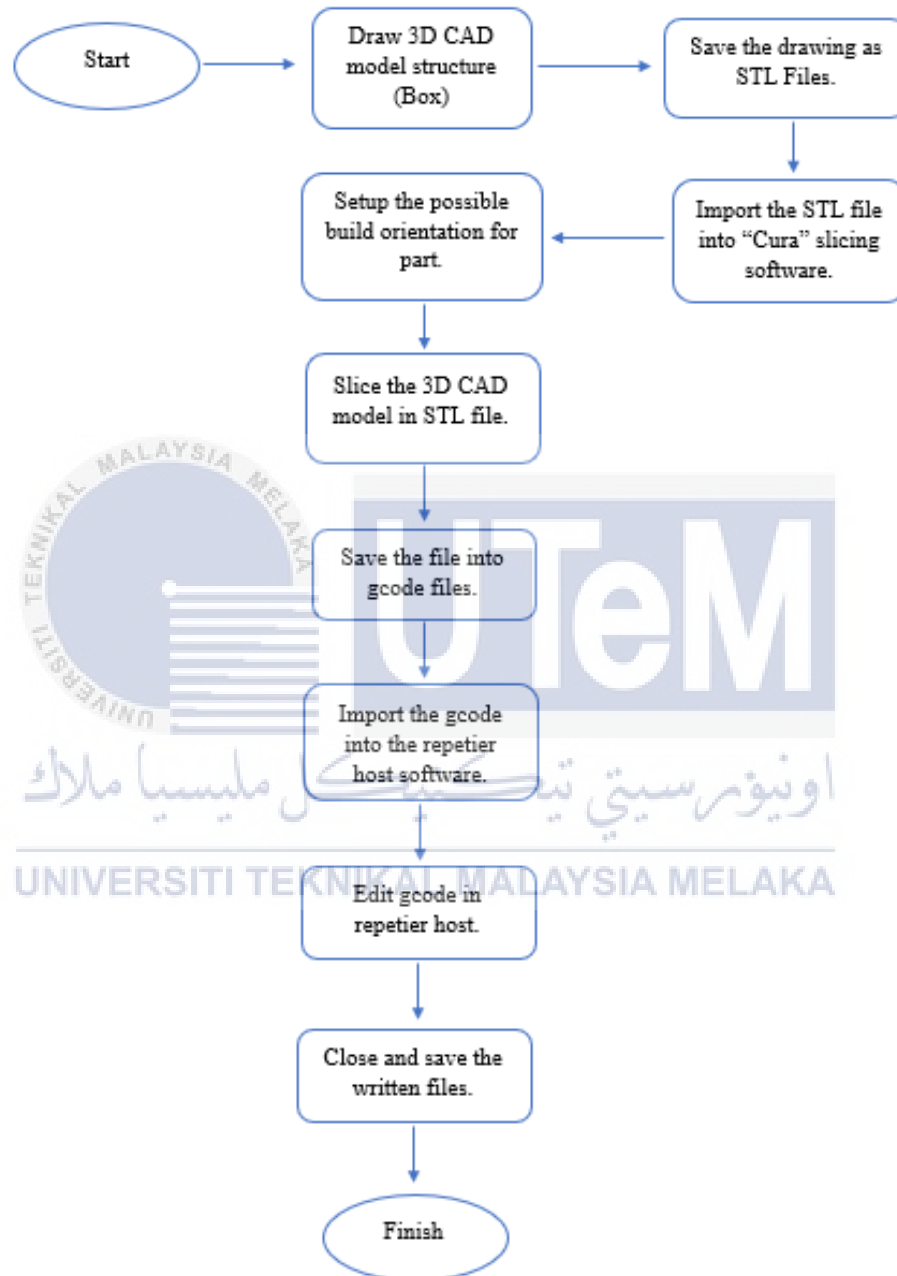


Figure 3.2: Wire arc additive manufacturing system

Firstly, the process starts with the draw of the 3D model structure such as box with the dimension of 50mm x 50mm x 30mm respectively. Then, the drawing file will be saved as STL

files to import into “Cura” slicing software. After that, in the “Cura” software setting, setup the possible build orientation for the model. Then, slice the model and save the file as G-code files. After that, import the gcode into the “Repetier Host” software to determine and edit the path planning of robot welding. Then, running the written files in ABB “RobotStudio” software to determine whether the G-code files can be run smoothly or need to edit the parameter in the “Cura” slicing software. Lastly, the fabrication of the 3D model structure will begin until the model finish weld.

### **3.5 Equipment used.**

The equipment should be prepared before starting the project. The equipment that been used in this project are the “Cura” software, SolidWorks, “Repetier Host” software and robotic arm welding ABB “IRB 1410 M2004”. “Dassault Systèmes” created the popular computer-aided design (CAD) programme called “SolidWorks”. For designing and modelling 3D parts, assemblies and drawings, it offers a complete set of tools. To assist in the design and development process, SolidWorks provides a user-friendly interface, robust parametric modelling capabilities and a variety of analysis tools so that it can draw the 3D model structure for this project. The popular open-source 3D printing slicing programme “Cura” was created by “Ultimaker”. By creating the required toolpaths and instructions for the 3D printer, it is made to get 3D models ready for printing. It became the mainly open-source software for this project because this software is free software that can be downloaded from the Internet. Popular open-source 3D printing software called Repetier-Host is used to operate and manage 3D printers. Users can slice 3D models, change print parameters, check the status of their prints, and manage print queues using Repetier-Host, which supports a variety of printer models. “Repetier Host” software is software that can generate the path planning of arc welding that was used in this project because it can edit the gcode and edit the starting point and end point. As for robotic arm welding, ABB Robotics created the ABB IRB 1410 M2004 robotic welding

system. It delivers excellent precision, flexibility, and dependability in the welding process and is intended for industrial welding applications. The IRB 1410 M2004 robot has cutting-edge features and capabilities that will increase welding operations' productivity and effectiveness.

### **3.6 Path planning flow for robot WAAM**

After importing the STL files into “Cura” slicing software, the printer will set up. Then, setup the printing setting in “Cura” software. Next, parameters will be inserted follows as welding setting and determine the path planning of the welding. After that, slice the 3D model structure and make sure it is not more than 5 layers. Lastly, save the files as G-codes files to import into the robot welding. Figure 3.3 shows the process of the “Cura” slicing software to determine the objective 1 for this project executed.



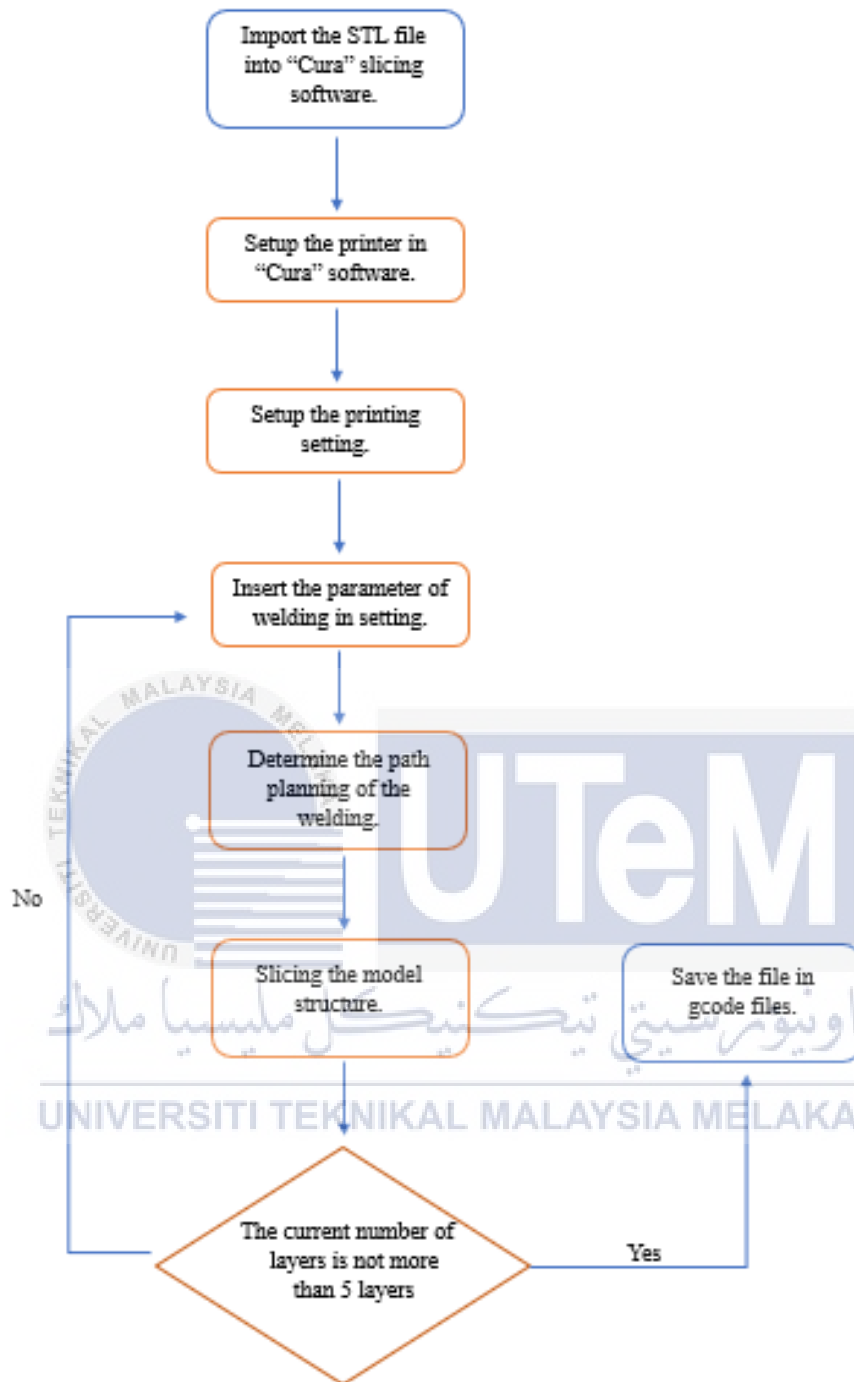


Figure 3.3: Slicing process using “Cura” slicing software

### 3.6.1 Parameter in the “Cura” software printing setting.

Parameter is a crucial factor to make the path planning of the robot welding to begin welding. In this study, the parameter in this “Cura” software had been setting in the printing setting section. First, the printer that had been used was “Creality Ender-5”. Then, import the

3D model from the STL files to generate the model structure in “Cura” software. Then, set its height each layer, thickness and wall thickness. Figure 3.4 shows the setting from the 3 parameters above.

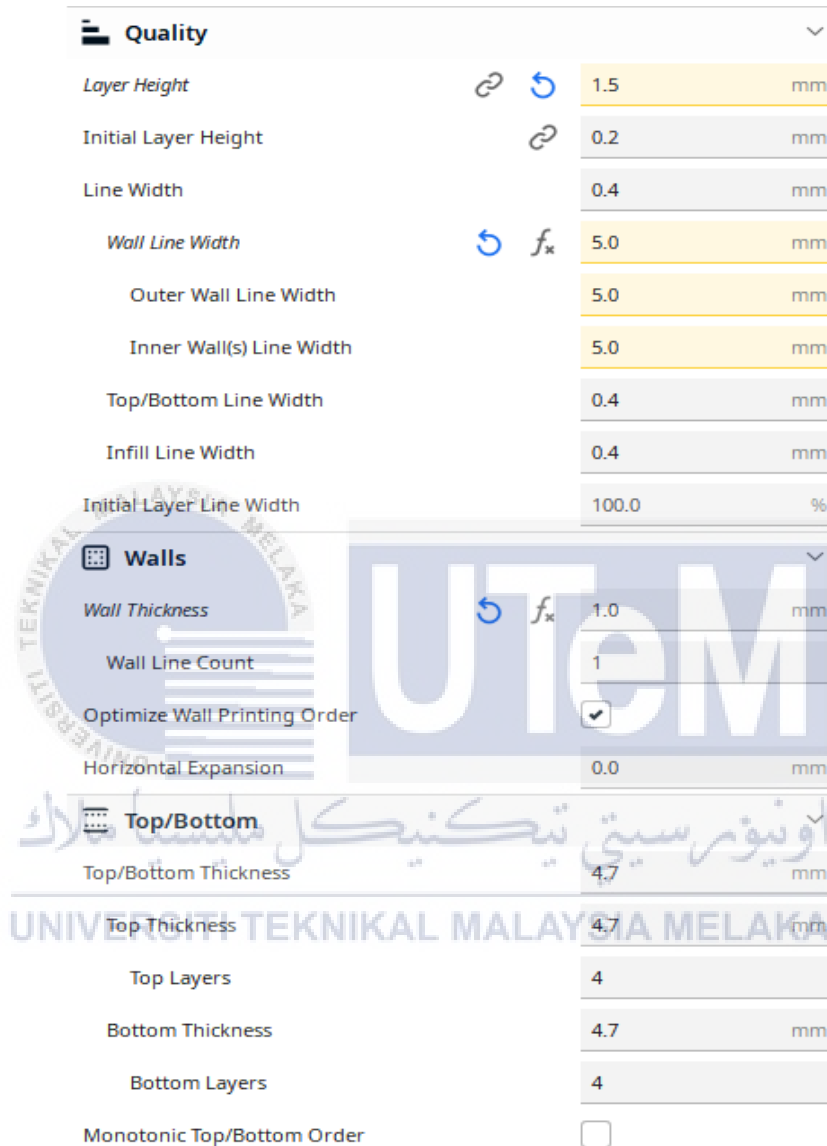


Figure 3.4: Parameter of each layer height, thickness and wall thickness

After that, the infill density will be 20% and the infill line distance is 6mm. For the pattern in this slicing, cubic pattern has been used to make a path planning and the infill layer thickness is 1.5 mm. The material for this printing is using PLA but for generate complex model in this project, stainless steel will used. As for the printing temperature, it will increase to 200

°C while for the build plate will increase until 50 °C minimum. Figure 3.5 illustrates the parameter of the infill density and the temperature of printing.

☒ Infill		
Infill Density	20.0	%
Infill Line Distance	6.0	mm
Infill Pattern	Cubic	▼
Infill Line Multiplier	1	
Infill Overlap Percentage	30.0	%
Infill Layer Thickness	1.5	mm
Gradual Infill Steps	0	
⊕ Material		
Printing Temperature	200.0	°C
Printing Temperature Initial Layer	200.0	°C
Initial Printing Temperature	200.0	°C
Final Printing Temperature	200.0	°C
Build Plate Temperature	50	°C
Build Plate Temperature Initial Layer	50	°C

Figure 3.5: Parameter of Infill density and temperature of printing

Then the speed of the extruder is 80 mm/s and for the wall speed is 40 mm/s. For the travel speed of the printing is 200 mm/s and the initial layer speed is 20 mm/s. For the travel section, retraction had been enabled and the retraction distance and speed will be set into 5.0 mm and 45.0 mm respectively. In the travel setting section, the travel avoid distance will be set to 0.625 mm because it will not overlap with the part that already printed. Figure 3.6 represents the parameter of speed section and travel section.

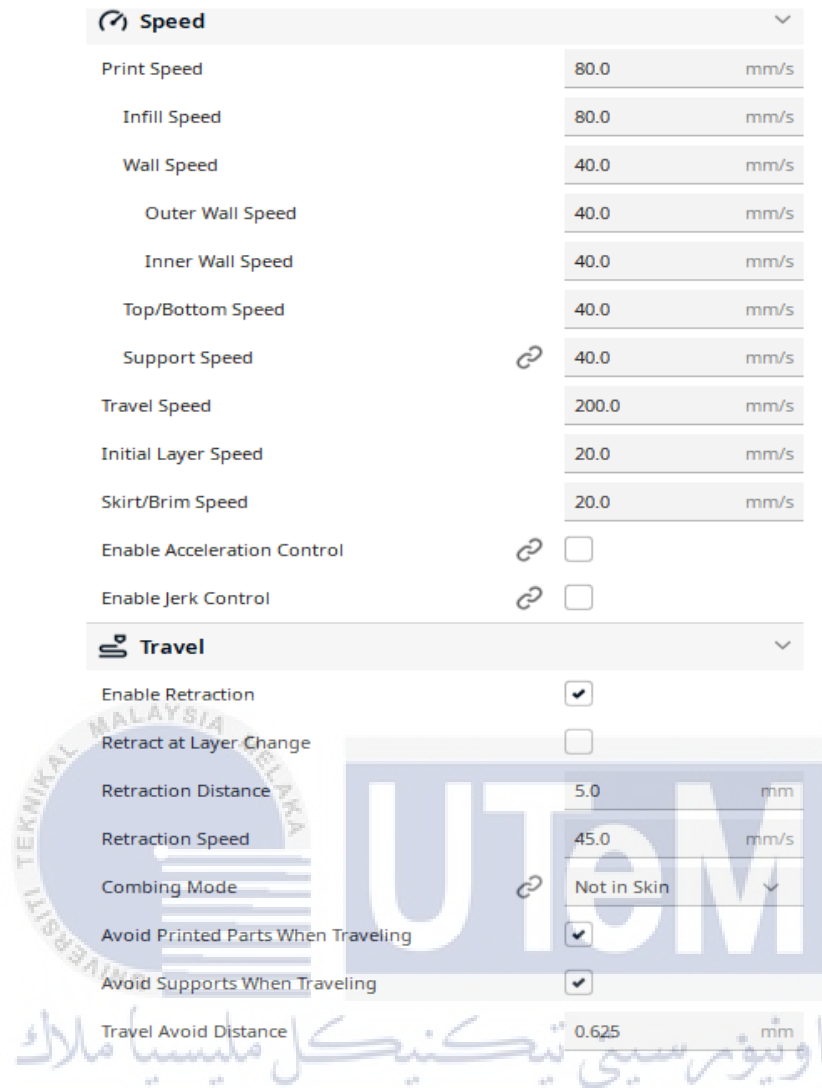


Figure 3.6: Parameter of the speed and travel printing

Lastly, the cooling setting will enable and the fan speed will use 100% of the max speed of fan and the regular speed/ maximum fan speed threshold is 10s. Additionally, the regular fan speed is at 3.2 mm height and the regular fan speed is at layer 4 and the minimum each layer 10s with the minimum speed at 10 mm/s. Figure 3.7 represents the parameter of the cooling section in the “Cura” software.

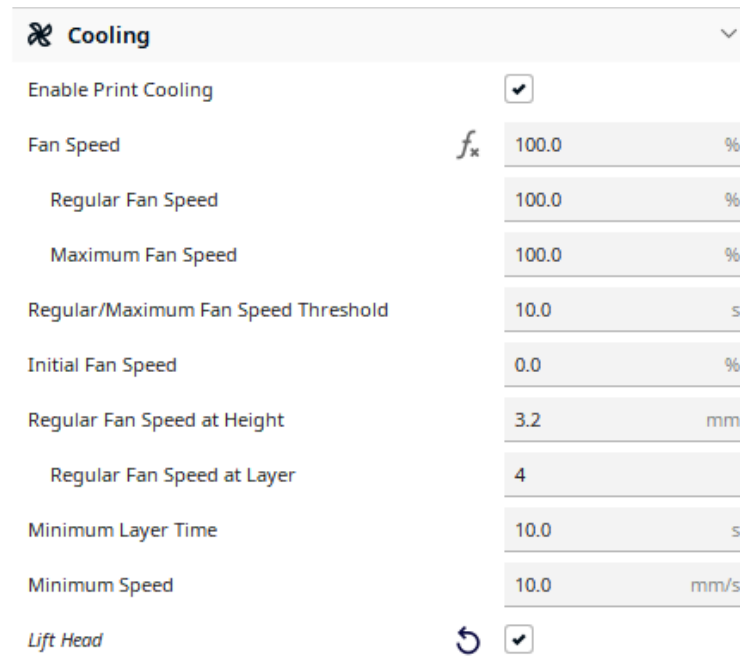


Figure 3.7: Parameter of cooling section printing

After that, the model will begin the slicer and path planning and will be saved into the gcode files. Figure 3.8 shows the path planning and the model after slicing.

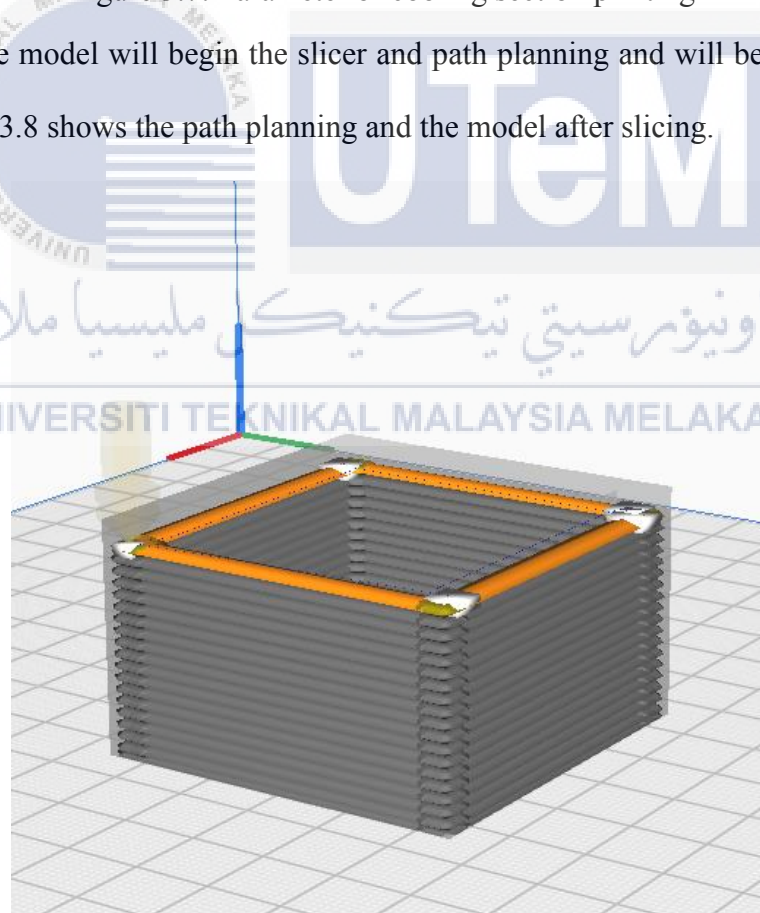


Figure 3.8: The model after slicing begins and path planning shown

### 3.7 Fabrication of 3D structure

Although the fabrication can yield positive results and optimize the entire experiment, a welding experimental design must first be developed. These include the 3D model design, fitting-up process, the welding process, the cleaning process and the preparation of the welding materials.

#### 3.7.1 Design of 3D model

The design of the 3D model had been drawn by SolidWorks software. Figure 3.9 illustrates the 3D model that has been created with the dimensions.



Figure 3.9: 3D model structures with dimensions

#### 3.7.2 Material preparation

Figure 3.10 shows the substrate plate as the material preparation to fabricate the model. Mild steel plate was used as substrate plate.



Figure 3.10: Material preparation (Mild steel plate)

### 3.7.3 Fit Up process.

The material chosen must be free of corrosion and other contaminants. The material's dimensions should be precisely as specified. Size-wise, it measures 100mm in length, 100mm in width, and 6mm in thickness. The wire feeder unit uses 1.0 mm copper wire as the material substrate. Figure 3.11 depicts a schematic of the entire substrate plate fit up procedure, and Figure 3.12 shows a diagram of the wire feeder unit.

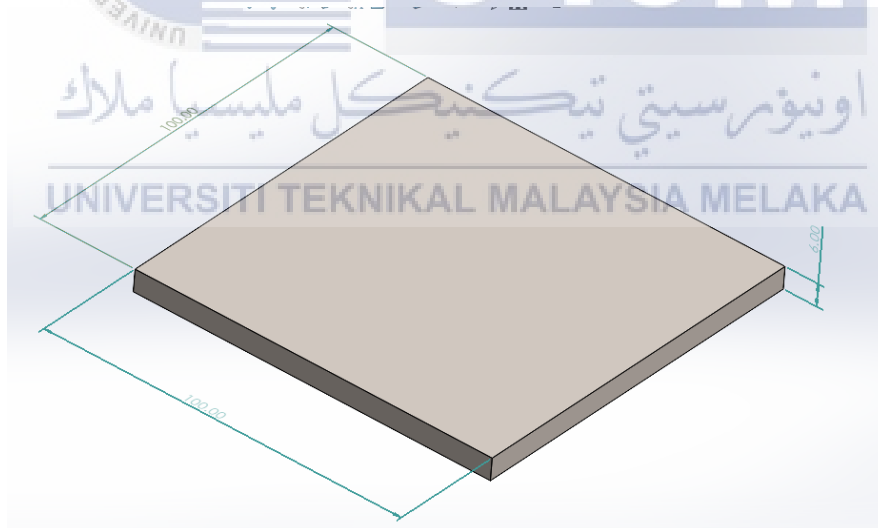


Figure 3.11: Overview of substrate plate fit up process with dimension



Figure 3.12: Wire feeder unit Copper coated ER70S-6 Ø 1.0 mm

#### 3.7.4 Machine preparation

The welding robot employed in the MIG-WAAM process is manufactured by ABB Engineering (Shanghai) Ltd. The robotic device in question belongs to the IRB 1410 M2004 category, with a specific model type of IRB 1410-5/1.45. The power supply in use is the Kemp arc Pulse 350, which provides a power range of 20A/12V to 350A/34V. The power generator produces an output of 3 x 400V in voltage, with a frequency range of 50-60 Hz. It has a rated current of 7A and a short circuit current of 6.5 A. The welding robot utilized in this experiment is depicted in Figure 3.13, manufactured by ABB. The chemical composition of the subject is presented in Table 5. The Copper coated wire was selected due to its extensive usage in the welding industry for diverse industrial purposes, including structural steel components, automobile bodies and pipes. It is frequently accessible in workshops. The materials utilized as substrates for the welding deposition process consisted of two mild steel plates, each measuring 100 mm x 100 mm x 6 mm. The welding torch's movements are governed by a six-axis robot. During the welding procedure, a shielding gas consisting of 100% Argon was employed, with a flow rate ranging between 15-20 L/min. The selection of 100% Argon gas

for shielding during welding was based on its cost-effectiveness and ability to facilitate deep penetration. This gas is frequently encountered in industrial settings claims Le et al. in 2020.



Figure 3.13: IRB 1410 M2004 robot welding

Table 5: Chemical composition of the ER70S-6 wire in weight percentage(%), source (Merbin et al., 2021)

Element	C	Si	Mn	P	S	Ni	Cr	Mo	Cu	V
Standard	0.06- 0.15	0.80- 1.15	1.40- 1.85	0.025	0.035	0.023	0.051	0.15	0.50	0.03
Typical	0.10	0.88	1.56	0.011	0.012	0.01	0.02	<0.01	0.24	<0.01

### 3.7.5 Welding process

Coordination is necessary for the preparation of welding projects. Welding parameters and equipment utilisation are included in the programmed specifications. The purpose of welding parameters is to ensure that the correct equipment is used, that the welding method adheres to specifications, and that the machine is operated in the proper sequence. On the substrate, the deposition direction is utilised to produce a thin-walled sample. The order of each layer of welding is maintained. When the deposition is complete, the torch is moved to the

beginning of the next deposition, and an idle cooling temperature between 150 and 350 degrees celsius is used to chill the wall between two adjacent layers in accordance with previous research (Knezovi et al., 2020). This experiment employs a welding current  $I$  (A) of 138 amps. The voltage (V) 19 volt. Before beginning, jog the robot planning with repeated layers and cycles of weld and 21 layers and cubic pattern with the same parameters to identify path planning errors. The recommended arc distance between infill wire and base metal is 2-3 mm. The voltage and speed of the wire feed may need to be adjusted based on the appropriateness of the current discovered in the table during the operation. The model and substrate were chilled to room temperature upon completion of the construction of the box model.

### **3.7.6 Pre-cleaning**

Following the completion of the welding procedure, the sample should be cleaned. Cleaning is performed both in and around the welding area. This process is carried out as a preliminary step prior to the visual test. One of the requirements is that the welding area be free of splashes and that there be no oil on the welding surface. Furthermore, any contaminants on the welding surface or in the surrounding region are thoroughly cleaned so that they do not interfere with the procedure during the visual test.

### **3.7.7 Observation method**

Observation method is a fundamental method that is used to evaluate the quality and integrity of an item or material by visually evaluating the surface or other exterior elements of the item or substance. The human eye and the ability to observe are utilised in this method to identify any faults, irregularities, or anomalies that are visible and may have an impact on the functionality or look of the item that is being inspected. Depending on the level of attention to detail that is required, observation may be performed with or without the assistance of tools such as magnifying lenses or inspection lamps. During the observation, the inspector performs

a thorough examination of the surface of the object, looking at it from a variety of perspectives and under varying lighting circumstances to ensure that they have the best possible visibility. The procedure entails inspecting the component for a variety of flaws, such as cracks, scratches, dents, corrosion, discolouration, incomplete welds, porosity or any other apparent indicators of damage or divergence from the specified requirements. It is the first stage of quality control, and its purpose is to enable the detection of obvious flaws or anomalies that may require more investigation or corrective actions.



## CHAPTER 4

### RESULTS AND DISCUSSION

#### 4.1 Introduction

This chapter explained the outcome of the production of the single line layer and the production of complex model. The framework was depicted and compared to the design generated by CAD and Slicer. Each robot engaged in welding was programmed with instructions to enable it to acquire path planning skills for fabricating the model. The single line layer was built to evaluate the success and visual appeal of both parameters by utilizing two input variables. The complex model was produced using the most suitable set of parameters. The resulting output serves as evidence to determine whether the parameters can successfully construct a 5-layer complex model. The ongoing discussion of the results described the limitations and flaws that arise during the fabrication process.

#### 4.2 Printing setting path planning flow for robot WAAM

In order to construct 3D metal structure by WAAM method, the required route planning flow using open-source software to simplify the process and minimizing the cost. The process as described in Figure 4.1. Firstly, the CAD model was drawn using SOLIDWORK 2017 with the dimension of the 50 mm x 50 mm x 10 mm as a recommendation or designated to compare with the other method. After that, complex model placed into "Cura" slicer in the format STL files because Cura slicer can read the data in the STL files alone. Next, the printer had been configured into Creality Ender 5 printer owing to the more stable at high speed and trial of the printing setting were done to acquire the optimal criterion of parameters. When the model had been produced with the ideal selection

printing setting, the slice began to check whether it follow the criteria of WAAAM and been saved in G-code files. Lastly the G-code modified at the start and the finished based on the robot welding constraints via Repetier-Host Software V2.3.1. After that, the fabrication began to construct the model as a prove the productively of the path planning development.



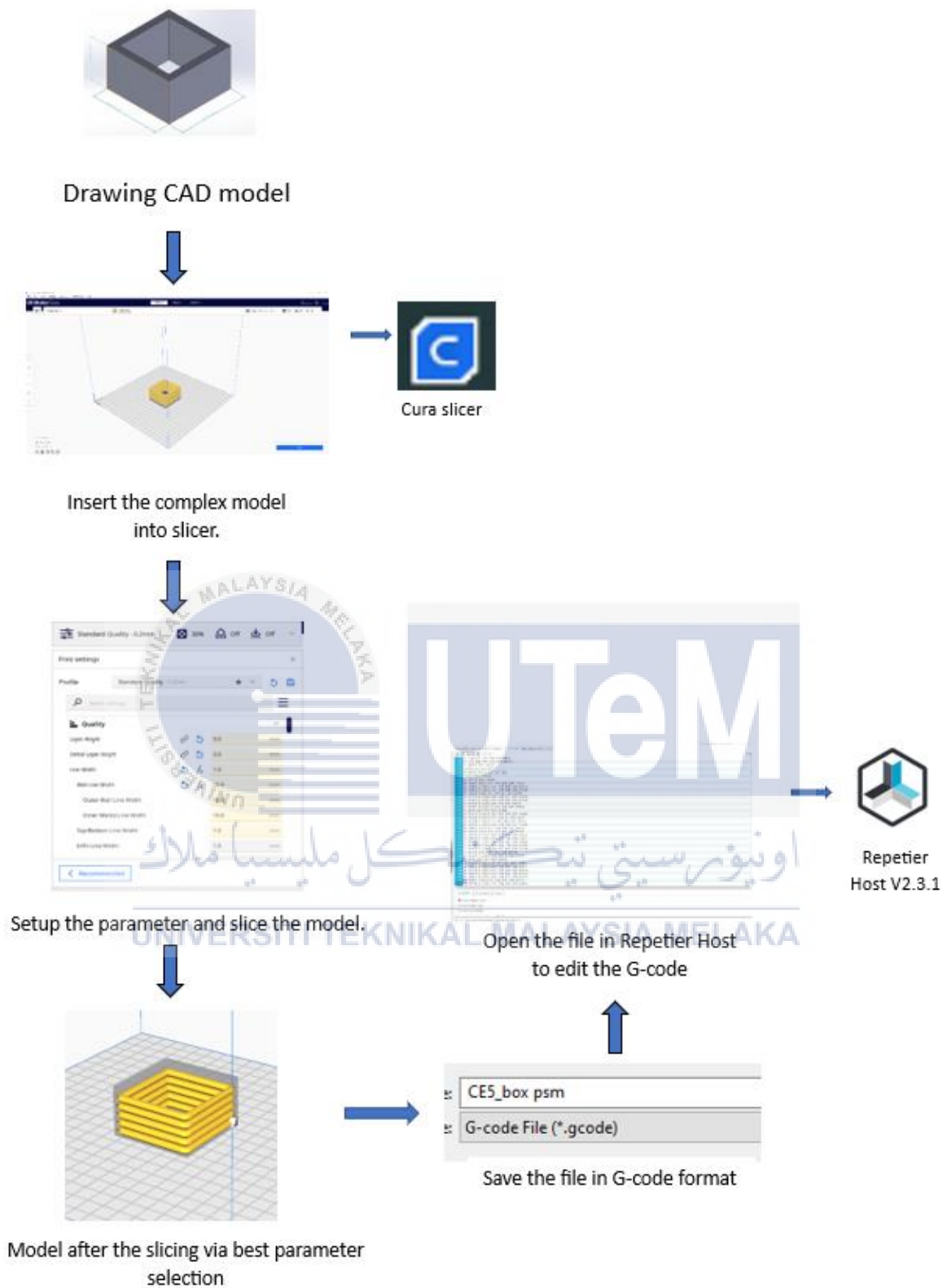


Figure 4.1: Path planning flow for slicer.

### **4.3 Single layer deposition.**

Single-layer deposition in the context of additive manufacturing refers to the technique of systematically adding material to build up a three-dimensional object one layer at a time. This technology is a basic part of numerous additive manufacturing techniques, including technologies like 3D printing and Wire Arc Additive Manufacturing (WAAM). In single-layer deposition, each horizontal cross-section of the object is formed individually and piled onto the preceding layers until the entire structure is complete.

In the case of WAAM, which utilizes arc welding with metal wire, single-layer deposition involves the controlled melting and deposition of metal in a precise path depending on the design of the 3D model. This layer-by-layer method enables for the production of complicated and customized components with precision. The capacity to add material selectively in a controlled manner during each layer contributes to the efficiency, flexibility and intricacy achievable in the production process. For this process, single layer deposition had been developed to determine the optimal parameter using path planning flow of WAAM process.

#### **4.3.1 Result of the fabrication of the single line layer.**

Based on the diagram shown in figure 4.2, the CAD model was created with a single line of 150 mm in length. The CAD drawing provides a clear representation of the dimensions of the single line layer. The path planning algorithm for the slicer model has been developed and implemented in the code, taking into account the selected parameters for the robot welding arm machine. Nevertheless, the fabricate model provides an explanation of the product of the line layer for comparison with the slicers and the CAD model to ensure accurate execution of the same output. The CAD and slicing model have

been utilized as indicators for fabricating the model layer by layer. This framework was developed to ascertain the parameters of the intricate model.

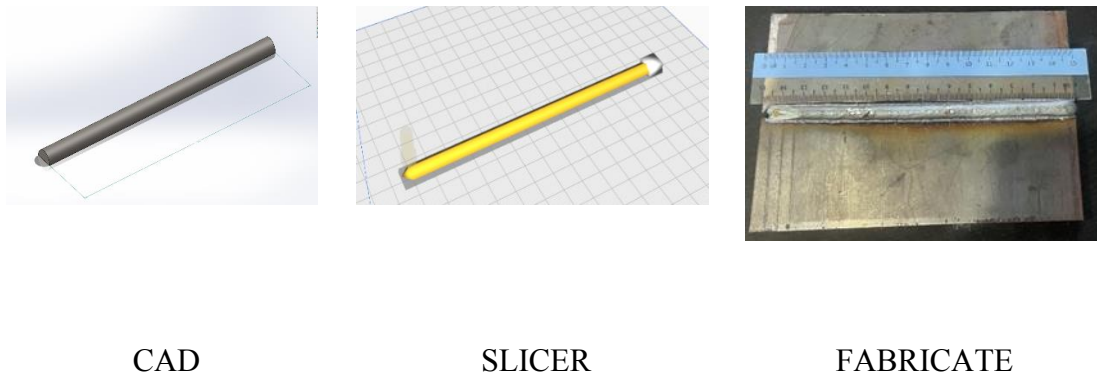


Figure 4.2: Different framework of the single line model

#### 4.3.2 Coding for single line based on the slicer model.

The slicing software dissects the 3D model into numerous horizontal layers and determines the toolpath that the 3D printer's nozzle or head will follow for each layer. This software considers various parameters such as layer thickness, printing speed, infill density and temperature settings to optimize the printing process. The generated G-code comprises a series of precise instructions for the printer, encompassing movements along the X, Y and Z axes, extrusion rates for depositing material, temperature control for the printing bed and nozzle, retraction for filament handling. As shown in **Appendix B**, the coding for the single line layer had been executed and from that it determined the direction of the deposited layer.

#### 4.3.3 Command of controller robot welding arm.

LABEL OF COMMAND	REFER TO
A	Appendix C
B	Appendix D

The command developed from the pendant controller of the robot welding arm and was referenced to APPENDIX C. This command was executed to enable the robot arm to acquire the movement pattern of the trajectory, starting at the initiation of the weld and continuing until its completion. APPENDIX D provides a detailed explanation of the command used to control the mobility of the deposited layer during welding. The command B yields the same deposited direction as command A, but it is directed in the other way. Thus, this instruction enables the robot to execute movement based on the specified command and specifies the timing of the arc weld.

#### 4.3.4 Comparison of the command of the robot welding arm.

Table 6: Comparison of the command robot welding

Command 1	Command 2
Different speed travel	
Same deposited direction but opposite direction with other command.	
Different height of torch and plate	

The differences between these two directives lies in the varying speed at which they move. The difference in speed between these two orders is a significant contributing element. The disparity in elevation between the torch and plate is also one of the factors that influence the final outcome. Nevertheless, these orders had the same deposited orientation because to the utilization of the same slicer G-code. However, the deposited layer of one command was in the opposite direction compared to the other command.

#### 4.3.5 Analysis of single layer deposition.

Table 7: Analysis of single line layer deposition parameters.

Label	Welding Speed Rate (mm/s)	Wirefeed Rate (m/min)	Height Torch (mm)	Voltage (V)	Current (A)	Weld width (mm)
A	200	10	5	19	138	10
B	300	10	5	18	138	11

WAAM entails the meticulous management of critical settings and variables, referred to as parameters, that are essential for the exact layer-by-layer deposition process. The parameters encompass various factors, including welding current, voltage, arc length, travel speed, wire feed rate. Each metric has a crucial role in determining the quality, structural integrity, and characteristics of the product. The parameters are meticulously adjusted and fine-tuned to regulate the level of thermal energy, rates of material deposition, flow of materials, and environmental circumstances. Achieving the ideal balance and fine-tuning of these parameters is essential for producing components with precise geometries, outstanding mechanical properties, and minimized defects. The process of optimization in additive manufacturing often involves a repetitive sequence of experimentation, monitoring, and correction in order to achieve the desired outcomes for specific materials and applications. Table 7 illustrates the range of parameters employed in the fabrication of the single line.

#### 4.3.6 Observation Test Result

Observation test is the one of act of assessing an object, component, product or system using human vision to evaluate its characteristics, properties, quality and adherence to particular standards or criteria. Observation test is conducted to identify any abnormalities, faults, deviations or irregularities that could impact the item's functioning, performance or attractiveness. This inspection approach utilizes visual observation and

expert knowledge to detect apparent defects, guaranteeing that products adhere to predetermined criteria or standards prior to being delivered to clients or progressing in the production workflow.

#### 4.3.7 Observation test for parameter A.

Table 8 shows the welding parameter used and Figure 4.3 shows a result picture of welding parameter A.

Table 8: Welding parameter of Parameter A

Label	Welding Speed Rate (mm/s)	Wire feed Rate (m/min)	Height Torch (mm)	Voltage (V)	Current (A)	Weld width (mm)
A	200	10	5	19	138	10



Figure 4.3: Picture of the welding parameter A

The single line layer was produced by utilizing the given parameter. Figure 4.3 depicts a visual representation of the welding process, utilizing parameter A. The figure

above illustrates that the deposited layer was executed in a left-to-right direction close the center of the plate. Based on a visual examination of the parameter A product, the presence of weld spatter is evident in the vicinity of the welding area. This is due to the minor increase in current consumption and arc speed. The welding result displays no discernible flaws on the welded surface. Welding spatter occurs when tiny fragments of metal are ejected during the process of arc or gas welding. These particles are excluded from the current weld. Welding spatter appears as small, luminous cylindrical imperfections on the surface.

#### 4.3.8 Observation test for parameter B

Table 9 show the welding parameter used and Figure 4.4 shows a result picture of welding parameter B.

Table 9: Welding parameter of parameter B

Label	Welding Speed Rate (mm/s)	Wire feed Rate (m/min)	Height Torch (mm)	Voltage (V)	Current (A)	Weld width (mm)
B	300	10	5	18	138	11



Figure 4.4: Picture of the welding parameter B

As shown in the Figure 4.4, the product had been fabricated. A lot of spatters can be seen around the weld area entirely according to the visual test performed on the parameter B. This is also in line with the results observed in parameter A, where the current consumption and arc distance exhibit a pretty significant magnitude. An observable flaw is the presence of porosity on the surface of the weld. This occurs due to the entrapment of gas during the process of solidification of the metal. Porosity is often indicated by the presence of small holes or dark, spherical or irregular spots. These might appear alone, in clusters or in linear formations.

#### 4.3.9 Overall summary of the two parameters

Table 10: Table of the welding defects with the Visual result

PARAMETER	DEFECTS	DIMENSIONS	ACCEPTANCE CRITERIA	RESULT
A	Spatter	Surrounded area	Note: Must be removed	Acceptable

B	Spatter	Surrounded area	Note: Must be removed	Acceptable
	Partial under fill	Height of layer below 1.5 mm	Decrement not below 1.2 mm	Acceptable
	Overlap	At initial 4 mm	Not exceed 1.5 mm height.	Acceptable

*All dimension in: MM*

The table 10 describes the welding defects that occurred in both parameters model. For parameter A, the common defects that always occurred in weld is spatter. The spatter a spread surrounded area of the weld. So, it must be removed to meet the acceptance criteria and it is acceptable for the model to fabricate. As for parameter B, it also had the spatter defect because of the current consumption and the welding speed rate are slightly high. Partial under fill defect had been determined because the layer had slightly decrement but not exceed 1.2 mm so it is acceptable for the result. The overlap also occurred at initial 4 mm when deposited layer in performing the weld arc. In conclusion, both parameters meet the requirement of the acceptance criteria.

#### 4.3.10 Chosen of optimal parameter of single layer deposition.

Table 11: Best selection of the parameter for single line layer

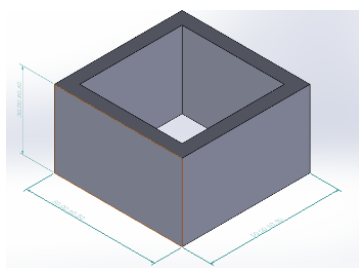
Label	Welding Speed Rate (mm/s)	Wire feed Rate (m/min)	Height Torch (mm)	Voltage (V)	Current (A)	Weld width (mm)
A	200	10	5	19	138	10

The most suitable parameter option for a single line layer is shown in Table 11. Parameter A is the optimal choice because it has the capability to minimize flaws throughout

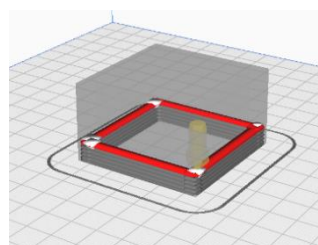
the continuing manufacturing process. Hence, this parameter is the most suitable choice for developing the complex model.

#### 4.4 Fabrication of the 3D complex model.

The CAD model is a representation of the product or component that was made using the software "SolidWorks". The description outlines the most notable attributes, including accurate geometry and dimensions. The engineers utilized the CAD model to create and simulate goods prior to the commencement of production. The slicer model analyzes the CAD model and produces the G-code for robot welding. The purpose of the slicer model was to dissect the CAD model into individual layers and decide the path planning for the construction of the final product, which occurs layer by layer. It is employed in robot welding or any process that constructs objects layer by layer based on a digital model. The constructed model was produced to demonstrate that it meets the standards of several models. Ultimately, the product serves as evidence of the design that has been developed to meet the specified requirements and slicing code. Every model played a crucial role in the product development or manufacturing process, guaranteeing the precise and efficient transformation of a concept into a tangible reality. Figure 4.5 displays the structure of the three complex models in various applications.



CAD



SLICER



FABRICATE

Figure 4.5: Framework of the complex model

#### 4.4.1 Coding for the complex model

The code was executed in the slicer and G-code was created using Repetier Host V2.3.1 software to determine the coordinates of the weld's starting and stopping points.

#### 4.4.2 Command of the robot welding for complex model.

The command for the complex model has been prepared and can be found in APPENDIX E. This command has been divided into five different layers. Every command specifies the path planning for the layer being deposited. Result of the best parameter were used for complex model.

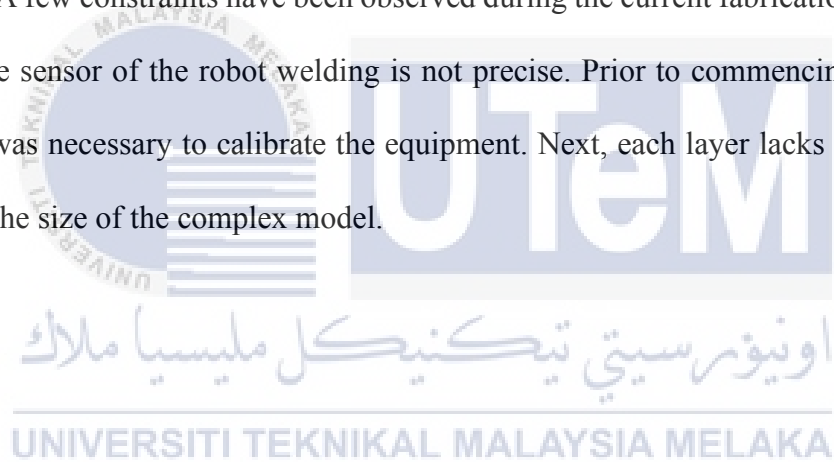


Figure 4. 6: Fabrication of complex model

As depicted in Figure 4.6, the fabrication has successfully fulfilled the parameter conditions. The model has a height of 5 layers, with dimensions of 50 mm x 50 mm x 10 mm. Nevertheless, it exhibits certain unavoidable flaws like as spatter, porosity, lack of fusion, sagging, and underfilled weld faults. This is due to the influence of the height of each layer on the complicated model and the cooling time after the proceed to the next layer.

#### 4.4.3 Discussion and evaluation of the 3D complex model.

To summarize, there has been thorough deliberation regarding several factors, such as the distance between the torch and the plate, the amount of time required for each layer to cool down after being fabricated, and the width of the weld. The height between the torch and the plate significantly affects the trajectory followed by the welding robot. Uneven height disparities among layers might lead to mistakes. The production process lacks an adequate amount of buffer time. The duration for each layer is unspecified. The experiment entails incorporating a 15-to-20-minute interval for cooling between the construction of each layer. As a result, several imperfections such as sagging, porosity, and poor filling developed. A few constraints have been observed during the current fabrication process. For instance, the sensor of the robot welding is not precise. Prior to commencing the welding process, it was necessary to calibrate the equipment. Next, each layer lacks the extent that influenced the size of the complex model.



## CHAPTER 5

### CONCLUSION AND RECOMMENDATIONS

#### 5.1 Conclusion

To properly accomplish this research, three objectives must be met within the span of the three research stages. The fabrication had been done using the right technique and proper usage of the equipment and material based on the scope investigation. Next, these tests had been done to produce sufficient proof to support the result of the research. To meet the objective one, the path planning has been discovered inside the parameter of the printing setup. Therefore, the path planning had a lot of variation setting to build great path planning for the complex model. As for the objective two, a lot of trial had been done to acquire these result and a variety of limitation of the robot welding that cannot be avoided. Therefore, in this experiment, the optimal selection of parameter had been achieved from the single line layer to used into the fabrication of the complex model. From that, the complex model had been developed and a lot of debate had been discuss to improvised the structure of the complex model that achieved the objective three. Finally, command of the robot welding had been achieved and the coding of the path planning from slicer is the evidence that prove the path planning succesfully obtained.

#### 5.2 Recommendations

In considering the study conducted on the "Development Path Planning of Wire Arc Additive Manufacturing Robotic System Based on Open-Source Software," a number of ideas emerge for both academics and industry. Firstly, it is advisable for academics and practitioners in the field of additive manufacturing to embrace and further explore the

utilization of open-source software, given its potential to promote accessibility, collaboration, and customization within the creation of robotic systems. Open-source platforms enable a collaborative environment for continual improvement and innovation.

Moreover, considering the dynamic nature of both additive printing and robots, continuous research efforts should focus on refining and expanding the capabilities of the open-source software utilized in path planning. This includes fixing any current constraints, upgrading user-friendly interfaces, and implementing new algorithms for more complicated trajectory optimization. Collaborative activities across the academic and industrial sectors can allow the sharing of knowledge, best practices, and the creation of standardized techniques.

Additionally, firms participating in the adoption of robotic systems for wire arc additive manufacturing are encouraged to invest in training programs for staff. This guarantees that operators, engineers, and researchers has the essential skills to properly exploit the capabilities of open-source software in path planning. Training programs can bridge the gap between technology developments and practical implementation, enhancing the benefits of this new method.

### **5.3 Project Potential**

By employing open-source software, the initiative not only contributes to the growth of wire arc additive manufacturing but also provides doors for cooperation, accessibility, and creativity within the broader academic community. The use of open-source platforms in path planning provides for transparency, adaptability, and continual development, promoting a collaborative environment where researchers, developers, and industry professionals may collaboratively contribute to the progress of robotic systems.

The potential impact extends to industrial applications, where the suggested approaches can boost the efficiency and precision of wire arc additive manufacturing processes. Industries adopting robotic systems for additive manufacturing can benefit from the customisation and adaptability given by open-source software, resulting to cost-effective solutions and quicker innovation cycles. Moreover, the project's achievements may pave the way for the creation of standardized processes in wire arc additive manufacturing, ensuring a unified and compatible approach across diverse systems.

Furthermore, the project has the potential to encourage further research and development projects. As the findings contribute to the knowledge base of path planning in additive manufacturing robotics, it may encourage related studies, collaborations, and breakthroughs in the integration of open-source tools into varied production processes. The project's success could spark a broader shift toward open-source techniques in the creation of robotic systems, creating a culture of knowledge-sharing and community advancement.

In conclusion, the project has the potential to greatly impact the disciplines of additive manufacturing and robotics by increasing collaboration, innovation, and accessibility. Its conclusions may influence industry practices, motivate new research endeavors, and contribute to the continued evolution of manufacturing technologies.

## REFERENCES

- Li, C., Gu, H., Wang, W., Wang, S., Ren, L., Wang, Z., Ming, Z., & Zhai, Y. (2019, December 20). Effect of Heat Input on Formability, Microstructure, and Properties of Al-7Si-0.6Mg Alloys Deposited by CMT-WAAM Process. *Applied Sciences*, *10*(1), 70. <https://doi.org/10.3390/app10010070>
- Miao, Y., Wu, Y., Wang, Z., Zhao, Y., Li, C., & Liu, J. (2022, November 14). Process Stability and Material Properties of TC4 Alloy Welded by Bypass Current Hot Wire Plasma Arc Welding (BC-PAW). *Metals*, *12*(11), 1949. <https://doi.org/10.3390/met12111949>
- Schwab, S., Selin, R., & Voron, M. (2023, January 19). Welding materials for TIG welding, surfacing, and WAAM technology of titanium alloys. *Welding in the World*, *67*(4), 981–986. <https://doi.org/10.1007/s40194-023-01464-z>
- Wang, L., Zhao, P., Pan, J., Tan, L., & Zhu, K. (2020, November 19). Investigation on microstructure and mechanical properties of double-sided synchronous TIP TIG arc butt welded duplex stainless steel. *The International Journal of Advanced Manufacturing Technology*, *112*(1–2), 303–312. <https://doi.org/10.1007/s00170-020-06375-7>
- Ayarkwa, K., Williams, S., & Ding, J. (2017, December). Assessing the effect of TIG alternating current time cycle on aluminium wire + arc additive manufacture. *Additive Manufacturing*, *18*, 186–193. <https://doi.org/10.1016/j.addma.2017.10.005>
- Murali, P., & Gopi, R. (2021). Experimental investigation of tungsten inert gas welding (TIG) using Ar/Ar-CO<sub>2</sub> shielding gas on alloy steels. *Materials Today: Proceedings*, *39*, 812–817. <https://doi.org/10.1016/j.matpr.2020.09.776>
- Feier, A., Buta, I., Florica, C., & Blaga, L. (2022, December 20). Optimization of Wire Arc Additive Manufacturing (WAAM) Process for the Production of Mechanical Components Using a CNC Machine. *Materials*, *16*(1), 17. <https://doi.org/10.3390/ma16010017>
- Zhang, R. Y., Hu, Y. Y., & Wang, J. (2013, December). Research on the Technology for DC CMT Welding of AZ31B Magnesium Alloy. *Applied Mechanics and Materials*, *483*, 18–22. <https://doi.org/10.4028/www.scientific.net/amm.483.18>
- Madhavan, S., Kamaraj, M., Vijayaraghavan, L., & Srinivasa Rao, K. (2016, April 30). Microstructure and mechanical properties of aluminium/steel dissimilar weldments: effect of heat input. *Materials Science and Technology*, *33*(2), 200–209. <https://doi.org/10.1080/02670836.2016.1176716>
- Xin, Z., Yang, Z., Zhao, H., & Chen, Y. (2019, October 11). Comparative Study on Welding Characteristics of Laser-CMT and Plasma-CMT Hybrid Welded AA6082-T6 Aluminum Alloy Butt Joints. *Materials*, *12*(20), 3300. <https://doi.org/10.3390/ma12203300>
- Lei, Z., Li, B., Bi, J., Zhu, P., Lu, W., & Liu, J. (2019, December). Influence of the laser thermal effect on the droplet transfer behavior in laser-CMT welding. *Optics & Laser Technology*, *120*, 105728. <https://doi.org/10.1016/j.optlastec.2019.105728>
- Ding, M., Liu, S., Zheng, Y., Wang, Y., Li, H., Xing, W., Yu, X., & Dong, P. (2015, December). TIG–MIG hybrid welding of ferritic stainless steels and magnesium alloys with

Cu interlayer of different thickness. *Materials & Design*, 88, 375–383. <https://doi.org/10.1016/j.matdes.2015.09.022>

Ye, Z., Xie, L., & Huang, J. (2023, February 13). Al/steel joining by MIG welding with high frequency heating. *Materials and Manufacturing Processes*, 38(11), 1361–1371. <https://doi.org/10.1080/10426914.2023.2176871>

Gaur, V., Enoki, M., Okada, T., & Yomogida, S. (2018, February). A study on fatigue behavior of MIG-welded Al-Mg alloy with different filler-wire materials under mean stress. *International Journal of Fatigue*, 107, 119–129. <https://doi.org/10.1016/j.ijfatigue.2017.11.001>

Li, C., Duan, C. H., Qi, Y. C., Sun, Y. F., & Ma, C. Y. (2023, May). Effect of shielding gas on MIG welding performance with austenitic wire. *Materials Letters*, 339, 134118. <https://doi.org/10.1016/j.matlet.2023.134118>

Sameer S. Kulkarni et al., S. S. K. E. A. (2019). Optimization of Welding Parameters For MIG Welding of Al 6061-T6 Using Taguchi Technique. *International Journal of Mechanical and Production Engineering Research and Development*, 9(3), 695–704. <https://doi.org/10.24247/ijmperdjun201977>

Li, H., Liu, D., Yan, Y., Guo, N., Liu, Y., & Feng, J. (2018, January). Effects of heat input on arc stability and weld quality in underwater wet flux-cored arc welding of E40 steel. *Journal of Manufacturing Processes*, 31, 833–843. <https://doi.org/10.1016/j.jmapro.2018.01.013>

Xiong, J., Zhang, Y., & Pi, Y. (2020, July 24). Control of deposition height in WAAM using visual inspection of previous and current layers. *Journal of Intelligent Manufacturing*, 32(8), 2209–2217. <https://doi.org/10.1007/s10845-020-01634-6>

Yu, Y., Xue, X., Lu, Z., Li, T., Ma, C., Yan, P., & Yan, B. (2019, December 26). Effect of Mg plate pretreatment on microstructure and mechanical properties of Al/Mg/Al laminated composites fabricated by hot roll bonding. *International Journal of Modern Physics B*, 34(01n03), 2040052. <https://doi.org/10.1142/s0217979220400524>

Su, C., Chen, X., Gao, C., & Wang, Y. (2019, August). Effect of heat input on microstructure and mechanical properties of Al-Mg alloys fabricated by WAAM. *Applied Surface Science*, 486, 431–440. <https://doi.org/10.1016/j.apsusc.2019.04.255>

Prado-Cerqueira, J., Diéguez, J., & Camacho, A. (2017). Preliminary development of a Wire and Arc Additive Manufacturing system (WAAM). *Procedia Manufacturing*, 13, 895–902. <https://doi.org/10.1016/j.promfg.2017.09.154>

Dong, B., Cai, X., Lin, S., Li, X., Fan, C., Yang, C., & Sun, H. (2020, December). Wire arc additive manufacturing of Al-Zn-Mg-Cu alloy: Microstructures and mechanical properties. *Additive Manufacturing*, 36, 101447. <https://doi.org/10.1016/j.addma.2020.101447>

Klobčar, D., Lindič, M., & Bušić, M. (2018, December 1). Wire arc additive manufacturing of mild steel. *Materials and Geoenvironment*, 65(4), 179–186. <https://doi.org/10.2478/rmzmag-2018-0015>

- Xing, M. (2013). Competition between Free Open Source, Commercial Open Source and Proprietary Software. *Journal of Communications*, 8(10), 665–671. <https://doi.org/10.12720/jcm.8.10.665-671>
- Chen, C., He, H., Zhou, J., Lian, G., Huang, X., & Feng, M. (2022, December). A profile transformation based recursive multi-bead overlapping model for robotic wire and arc additive manufacturing (WAAM). *Journal of Manufacturing Processes*, 84, 886–901. <https://doi.org/10.1016/j.jmapro.2022.10.042>
- Kang, J., Shanguan, H., Deng, C., Hu, Y., Yi, J., Wang, X., Zhang, X., & Huang, T. (2018, August). Additive manufacturing-driven mold design for castings. *Additive Manufacturing*, 22, 472–478. <https://doi.org/10.1016/j.addma.2018.04.037>
- L. (2021, May 21). *Rope Access Work | Waterproofing Contractor*. Rope Access Work | Waterproofing Contractor. <https://waterproofing.com.sg/rope-access-work/>
- Qiu, C., & Liu, Q. (2019, December). Multi-scale microstructural development and mechanical properties of a selectively laser melted beta titanium alloy. *Additive Manufacturing*, 30, 100893. <https://doi.org/10.1016/j.addma.2019.100893>
- Asnafi, N. (2021, May 26). Metal Additive Manufacturing—State of the Art 2020. *Metals*, 11(6), 867. <https://doi.org/10.3390/met11060867>
- Wong, K. V., & Hernandez, A. (2012, August 16). A Review of Additive Manufacturing. *ISRN Mechanical Engineering*, 2012, 1–10. <https://doi.org/10.5402/2012/208760>
- Edgar, J., & Tint, S. (2015, July 1). “Additive Manufacturing Technologies: 3D Printing, Rapid Prototyping, and Direct Digital Manufacturing”, 2nd Edition. *Johnson Matthey Technology Review*, 59(3), 193–198. <https://doi.org/10.1595/205651315x688406>
- Derekar, K. S. (2018, April 8). A review of wire arc additive manufacturing and advances in wire arc additive manufacturing of aluminium. *Materials Science and Technology*, 34(8), 895–916. <https://doi.org/10.1080/02670836.2018.1455012>
- Snider-Simon, B., & Frantziskonis, G. (2022, March). Reliability of metal additive manufactured materials from modeling the microstructure at different length scales. *Additive Manufacturing*, 51, 102629. <https://doi.org/10.1016/j.addma.2022.102629>
- Rosli, N. A., Alkahari, M. R., Abdollah, M. F. B., Maidin, S., Ramli, F. R., & Herawan, S. G. (2021, March). Review on effect of heat input for wire arc additive manufacturing process. *Journal of Materials Research and Technology*, 11, 2127–2145. <https://doi.org/10.1016/j.jmrt.2021.02.002>
- Leitz, K. H., Singer, P., Plankensteiner, A., Tabernig, B., Kestler, H., & Sigl, L. (2017, September). Multi-physical simulation of selective laser melting. *Metal Powder Report*, 72(5), 331–338. <https://doi.org/10.1016/j.mprp.2016.04.004>
- Chen, H., Gong, Y., He, J., Qiao, Z., Hong, B., Li, W., Zhou, C., Zhou, R., & Shao, H. (2023, May 2). 3D Printing Process Research and Performance Tests on Sodium Alginate-Xanthan Gum-Hydroxyapatite Hybridcartilage Regenerative Scaffolds. *3D Printing and Additive Manufacturing*. <https://doi.org/10.1089/3dp.2022.0272>

- Petrik, J., Sydow, B., & Bambach, M. (2022). Beyond parabolic weld bead models: AI-based 3D reconstruction of weld beads under transient conditions in wire-arc additive manufacturing. *Journal of Materials Processing Technology*, 302, 117457. <https://doi.org/10.1016/J.JMATPROTEC.2021.117457>
- Duan, C., & Zhang, P. (2021). Path Planning of Arc Additive Remanufacturing for Defective Castings. *Proceedings - 2021 3rd International Conference on Artificial Intelligence and Advanced Manufacture, AIAM 2021*, 237–240. <https://doi.org/10.1109/AIAM54119.2021.00056>
- Ermakova, A., Mehmanparast, A., Ganguly, S., Razavi, J., & Berto, F. (2020). Investigation of mechanical and fracture properties of wire and arc additively manufactured low carbon steel components. *Theoretical and Applied Fracture Mechanics*, 109. <https://doi.org/10.1016/j.tafmec.2020.102685>
- Evans, S. I., Wang, J., Qin, J., He, Y., Shepherd, P., & Ding, J. (2022). A review of WAAM for steel construction – Manufacturing, material and geometric properties, design, and future directions. In *Structures* (Vol. 44, pp. 1506–1522). Elsevier Ltd. <https://doi.org/10.1016/j.istruc.2022.08.084>
- He, F., Yuan, L., Mu, H., Ros, M., Ding, D., Pan, Z., & Li, H. (2023). Research and application of artificial intelligence techniques for wire arc additive manufacturing: a state-of-the-art review. *Robotics and Computer-Integrated Manufacturing*, 82. <https://doi.org/10.1016/J.RCIM.2023.102525>
- Hu, Z., Liu, Y., Chen, S., Liu, S., Yu, L., Liu, Y., & Ma, Z. (2023). Achieving high-performance pure tungsten by additive manufacturing: Processing, microstructural evolution and mechanical properties. *International Journal of Refractory Metals and Hard Materials*, 113. <https://doi.org/10.1016/j.ijrmhm.2023.106211>
- Huang, C., Zheng, Y., Chen, T., Ghafoori, E., & Gardner, L. (2023). Fatigue crack growth behaviour of wire arc additively manufactured steels. *International Journal of Fatigue*, 173, 107705. <https://doi.org/10.1016/j.ijfatigue.2023.107705>
- Kalyankar, V. D., & Shah, P. (2018). A review on methodologies to reduce welding distortion. In *Materials Today: Proceedings* (Vol. 5). [www.sciencedirect.com/www.materialstoday.com/proceedings](http://www.sciencedirect.com/www.materialstoday.com/proceedings)
- Kozamernik, N., Drago Bračun, & Klobčar, D. (n.d.). *WAAM system with interpass temperature control and forced cooling for near-net-shape printing of small metal components*. <https://doi.org/10.1007/s00170-020-05958-8/Published>
- McAndrew, A. R., Alvarez Rosales, M., Colegrove, P. A., Hönnige, J. R., Ho, A., Fayolle, R., Eyitayo, K., Stan, I., Sukrongpang, P., Crochemore, A., & Pinter, Z. (2018). Interpass rolling of Ti-6Al-4V wire + arc additively manufactured features for microstructural refinement. *Additive Manufacturing*, 21, 340–349. <https://doi.org/10.1016/j.addma.2018.03.006>
- Niu, F., Bi, W., Zhang, K., Sun, X., Ma, G., & Wu, D. (2023). Additive manufacturing of 304 stainless steel integrated component by hybrid WAAM and LDED. *Materials Today Communications*, 35. <https://doi.org/10.1016/j.mtcomm.2023.106227>

- Ou, W., Mukherjee, T., Knapp, G. L., Wei, Y., & DebRoy, T. (2018). Fusion zone geometries, cooling rates and solidification parameters during wire arc additive manufacturing. *International Journal of Heat and Mass Transfer*, 127, 1084–1094. <https://doi.org/10.1016/j.ijheatmasstransfer.2018.08.111>
- Petrik, J., Sydow, B., & Bambach, M. (2022). Beyond parabolic weld bead models: AI-based 3D reconstruction of weld beads under transient conditions in wire-arc additive manufacturing. *Journal of Materials Processing Technology*, 302, 117457. <https://doi.org/10.1016/J.JMATPROTEC.2021.117457>
- Prakash, B., Rao, S. G. S., Gupta, S., Gupta, P., & Prasad, A. (n.d.). *Lecture Notes in Mechanical Engineering Advances in Engineering Materials*. <http://www.springer.com/series/11693>
- Rodrigues, T. A., Duarte, V., Miranda, R. M., Santos, T. G., & Oliveira, J. P. (2019). Current status and perspectives on wire and arc additive manufacturing (WAAM). *Materials*, 12(7). <https://doi.org/10.3390/ma12071121>
- Shukla, P., Dash, B., Kiran, D. V., & Bukkapatnam, S. (2020). *Arc behavior in wire arc additive manufacturing process*. 48, 725–729. <https://doi.org/10.1016/j.promfg.2020.05.105>
- Shukla, V., Kumar, V., & Dixit, A. (2023). Microstructural characteristics and tensile properties of ER70S-6 manufactured by Robotic CMT wire-and-arc additive manufacturing. *Materials Today: Proceedings*. <https://doi.org/10.1016/j.matpr.2023.02.011>
- Singh, J., Arora, K. S., & Shukla, D. K. (2020). Lap weld-brazing of aluminium to steel using novel cold metal transfer process. *Journal of Materials Processing Technology*, 283. <https://doi.org/10.1016/j.jmatprotec.2020.116728>
- Tankova, T., Andrade, D., Branco, R., Zhu, C., Rodrigues, D., & Simões da Silva, L. (2022). Characterization of robotized CMT-WAAM carbon steel. *Journal of Constructional Steel Research*, 199. <https://doi.org/10.1016/j.jcsr.2022.107624>
- Wang, X., Zhou, X., Xia, Z., & Gu, X. (2021). A survey of welding robot intelligent path optimization. *Journal of Manufacturing Processes*, 63, 14–23. <https://doi.org/10.1016/j.jmapro.2020.04.085>
- Wei, H. L., Mazumder, J., & DebRoy, T. (2015). Evolution of solidification texture during additive manufacturing. *Scientific Reports*, 5. <https://doi.org/10.1038/srep16446>
- Xu, F., Hou, Z., Xiao, R., Xu, Y., Wang, Q., & Zhang, H. (2023). A novel welding path generation method for robotic multi-layer multi-pass welding based on weld seam feature point. *Measurement: Journal of the International Measurement Confederation*, 216. <https://doi.org/10.1016/j.measurement.2023.112910>

## APPENDICES

### APPENDIX A: Gantt Chart

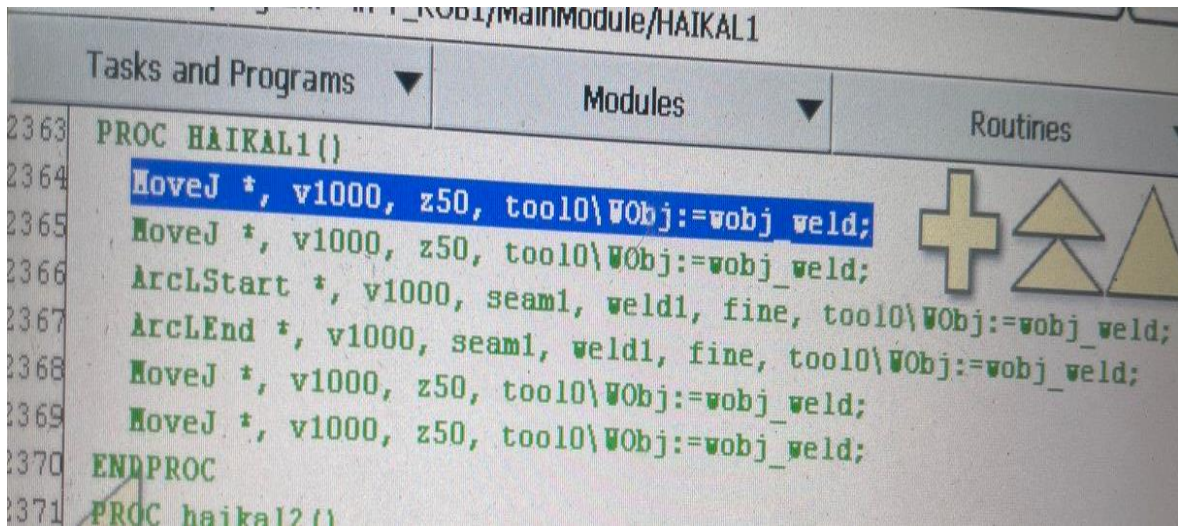
No	Task	PSM 1																PSM 2															
		Week																Week															
		1	2	3	4	5	6	7	8	9	10	11	12	13	14	15	16	17	18	19	20	21	22	23	24	25	26	27	28	29	30	31	32
1	Topic selection																																
2	Internet and library search																																
3	Idea sharing for project report																																
4	Preparation of chapter 1																																
5	Preparation of chapter 2																																
6	Preparation of chapter 3																																
7	Preliminary result																																
8	Progress with supervisor																																
9	Logbook and report PSM 1 to SV																																
10	Presentation and final PSM 1																																
11	Q and A with panel																																
12	Preparation of chapter 4																																
13	Preparation of chapter 5																																
14	Progress with supervisor																																
15	Logbook and report PSM 2 to SV																																
16	Presentation and final PSM 2																																
17	Q and A with panel																																
18	Report edits																																
19	Final submission																																

## APPENDIX B: Coding for single line layer

```
28 G92 E0 ;Reset Extruder
29 G1 Z2.0 F3000 ;Move Z Axis up
30 G1 X10.1 Y20 Z0.28 F5000.0 ;Move to start position
31 G1 X10.1 Y200.0 Z0.28 F1500.0 E15 ;Draw the first line
32 G1 X10.4 Y200.0 Z0.28 F5000.0 ;Move to side a little
33 G1 X10.4 Y20 Z0.28 F1500.0 E30 ;Draw the second line
34 G92 E0 ;Reset Extruder
35 G1 Z2.0 F3000 ;Move Z Axis up
36
37 G92 E0
38 G92 E0
39 G1 F180 E-5
40 ;LAYER_COUNT:1
41 ;LAYER:0
42 M107
43 M204 S500
44 ;MESH:Kaizer_single_line.STL
45 G0 F6000 X180.682 Y110 Z5
46 ;TYPE:WALL-OUTER
47 G1 F180 E0
48 G1 F1309.3 X39.318 Y110 E2537.78885
49 ;TIME_ELAPSED:61.422496
50 G1 F180 E2532.78885
51 M140 S0
52 G91 ;Relative positioning
53 G1 E-2 F2700 ;Retract a bit
54 G1 E-2 Z0.2 F2400 ;Retract and raise Z
55 G1 X5 Y5 F3000 ;Wipe out
56 G1 Z10 ;Raise Z more
57 G90 ;Absolute positioning
58
59 G28 X0 Y0 ;Present print
60 M106 S0 ;Turn-off fan
61 M104 S0 ;Turn-off hotend
62 M140 S0 ;Turn-off bed
63
64 M84 X Y E ;Disable all steppers but Z
65
66 M82 ;absolute extrusion mode
67 M104 S0
68 ;End of Gcode
```

APPENDIX C: Command A for single line layer

Command for Parameter A



```
2363 PROC HAICAL1()  
2364 MoveJ *, v1000, z50, tool0\WObj:=wobj_weld;  
2365 MoveJ *, v1000, z50, tool0\WObj:=wobj_weld;  
2366 ArcLStart *, v1000, seam1, weld1, fine, tool0\WObj:=wobj_weld;  
2367 ArcLEnd *, v1000, seam1, weld1, fine, tool0\WObj:=wobj_weld;  
2368 MoveJ *, v1000, z50, tool0\WObj:=wobj_weld;  
2369 MoveJ *, v1000, z50, tool0\WObj:=wobj_weld;  
2370 ENDPROC  
2371 PROC haikal2()
```



اونيورسيتي تيكنيكل مليسيا ملاك

UNIVERSITI TEKNIKAL MALAYSIA MELAKA

APPENDIX D: Command B for single layer

Command for Parameter B

```
PROC kal2()  
  MoveL *, v1000, z50, tool0\WObj:=wobj_weld;  
  ArcLStart *, v1000, seam1, weld1, fine, tool0\WObj:=wobj_weld;  
  ArcLEnd *, v1000, seam1, weld1, fine, tool0\WObj:=wobj_weld;  
  MoveL *, v1000, z50, tool0\WObj:=wobj_weld;  
  MoveL *, v1000, z50, tool0\WObj:=wobj_weld;  
ENDPROC
```



اونيورسيتي تيكنيكل مليسيا ملاك

UNIVERSITI TEKNIKAL MALAYSIA MELAKA

APPENDIX E: Command for complex model

First layer

```
PROC kal10()  
MoveJ *, v1000, z50, tool0\WObj:=wobj_weld;  
MoveJ *, v1000, z50, tool0\WObj:=wobj_weld;  
ArcLStart *, v1000, seam1, weld1, fine, tool0\WObj:=wobj_weld;  
ArcLEnd *, v1000, seam1, weld1, fine, tool0\WObj:=wobj_weld;  
MoveJ *, v1000, z50, tool0\WObj:=wobj_weld;  
MoveJ *, v1000, z50, tool0\WObj:=wobj_weld;  
MoveJ *, v1000, z50, tool0\WObj:=wobj_weld;  
ArcLStart *, v1000, seam1, weld1, fine, tool0\WObj:=wobj_weld;  
ArcLEnd *, v1000, seam1, weld1, fine, tool0\WObj:=wobj_weld;  
MoveJ *, v1000, z50, tool0\WObj:=wobj_weld;  
MoveJ *, v1000, z50, tool0\WObj:=wobj_weld;  
ArcLStart *, v1000, seam1, weld1, fine, tool0\WObj:=wobj_weld;  
ArcLEnd *, v1000, seam1, weld1, fine, tool0\WObj:=wobj_weld;  
MoveJ *, v1000, z50, tool0\WObj:=wobj_weld;  
MoveJ *, v1000, z50, tool0\WObj:=wobj_weld;  
MoveJ *, v1000, z50, tool0\WObj:=wobj_weld;  
ArcLStart *, v1000, seam1, weld1, fine, tool0\WObj:=wobj_weld;  
MoveJ *, v1000, z50, tool0\WObj:=wobj_weld;  
ArcLStart *, v1000, seam1, weld1, fine, tool0\WObj:=wobj_weld;  
ArcLEnd *, v1000, seam1, weld1, fine, tool0\WObj:=wobj_weld;  
MoveJ *, v1000, z50, tool0\WObj:=wobj_weld;  
MoveJ *, v1000, z50, tool0\WObj:=wobj_weld;  
ENDPROC
```

اوتور سیتی تکنیکل ملیسیا ملاک

UNIVERSITI TEKNOLOGI MELAKA LAYSIA MELAKA

Second Layer

```
PROC haikal4()  
MoveJ *, v1000, z50, tool0\WObj:=wobj_weld;  
MoveJ *, v1000, z50, tool0\WObj:=wobj_weld;  
ArcLStart *, v1000, seam1, weld1, fine, tool0\WObj:=wobj_weld;  
ArcLEnd *, v1000, seam1, weld1, fine, tool0\WObj:=wobj_weld;  
MoveJ *, v1000, z50, tool0\WObj:=wobj_weld;  
MoveJ *, v1000, z50, tool0\WObj:=wobj_weld;  
ArcLStart *, v1000, seam1, weld1, fine, tool0\WObj:=wobj_weld;  
ArcLEnd *, v1000, seam1, weld1, fine, tool0\WObj:=wobj_weld;  
MoveJ *, v1000, z50, tool0\WObj:=wobj_weld;  
MoveJ *, v1000, z50, tool0\WObj:=wobj_weld;  
ArcLStart *, v1000, seam1, weld1, fine, tool0\WObj:=wobj_weld;  
ArcLEnd *, v1000, seam1, weld1, fine, tool0\WObj:=wobj_weld;  
MoveJ *, v1000, z50, tool0\WObj:=wobj_weld;  
MoveJ *, v1000, z50, tool0\WObj:=wobj_weld;  
ArcLStart *, v1000, seam1, weld1, fine, tool0\WObj:=wobj_weld;  
ArcLEnd *, v1000, seam1, weld1, fine, tool0\WObj:=wobj_weld;  
MoveJ *, v1000, z50, tool0\WObj:=wobj_weld;  
ENDPROC
```

### Third layer

```
PROC haikal6()  
MoveJ *, v1000, z50, tool0\WObj:=wobj_weld;  
MoveJ *, v1000, z50, tool0\WObj:=wobj_weld;  
MoveJ *, v1000, z50, tool0\WObj:=wobj_weld;  
ArcLStart *, v1000, seam1, weld1, fine, tool0\WObj:=wobj_weld;  
ArcLEnd *, v1000, seam1, weld1, fine, tool0\WObj:=wobj_weld;  
MoveJ *, v1000, z50, tool0\WObj:=wobj_weld;  
MoveJ *, v1000, z50, tool0\WObj:=wobj_weld;  
MoveJ *, v1000, z50, tool0\WObj:=wobj_weld;  
ArcLStart *, v1000, seam1, weld1, fine, tool0\WObj:=wobj_weld;  
ArcLEnd *, v1000, seam1, weld1, fine, tool0\WObj:=wobj_weld;  
MoveJ *, v1000, z50, tool0\WObj:=wobj_weld;  
MoveJ *, v1000, z50, tool0\WObj:=wobj_weld;  
MoveJ *, v1000, z50, tool0\WObj:=wobj_weld;  
ArcLStart *, v1000, seam1, weld1, fine, tool0\WObj:=wobj_weld;  
ArcLEnd *, v1000, seam1, weld1, fine, tool0\WObj:=wobj_weld;  
MoveJ *, v1000, z50, tool0\WObj:=wobj_weld;  
MoveJ *, v1000, z50, tool0\WObj:=wobj_weld;  
ArcLStart *, v1000, seam1, weld1, fine, tool0\WObj:=wobj_weld;  
ArcLEnd *, v1000, seam1, weld1, fine, tool0\WObj:=wobj_weld;  
MoveJ *, v1000, z50, tool0\WObj:=wobj_weld;  
MoveJ *, v1000, z50, tool0\WObj:=wobj_weld;  
ENDPROC
```

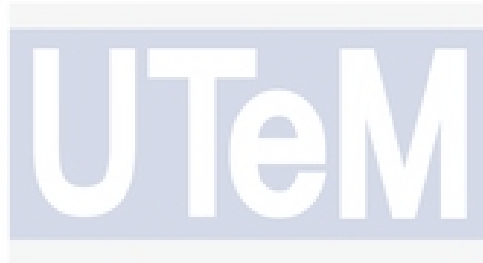
اونيورسيتي تيكنيكل مليسيا ملاك

### Fourth layer

```
PROC kal  
MoveJ *, v1000, z50, tool0\WObj:=wobj_weld;  
MoveJ *, v1000, z50, tool0\WObj:=wobj_weld;  
ArcLStart *, v1000, seam1, weld1, fine, tool0\WObj:=wobj_weld;  
ArcLEnd *, v1000, seam1, weld1, fine, tool0\WObj:=wobj_weld;  
MoveJ *, v1000, z50, tool0\WObj:=wobj_weld;  
MoveJ *, v1000, z50, tool0\WObj:=wobj_weld;  
ArcLStart *, v1000, seam1, weld1, fine, tool0\WObj:=wobj_weld;  
ArcLEnd *, v1000, seam1, weld1, fine, tool0\WObj:=wobj_weld;  
MoveJ *, v1000, z50, tool0\WObj:=wobj_weld;  
MoveJ *, v1000, z50, tool0\WObj:=wobj_weld;  
ArcLStart *, v1000, seam1, weld1, fine, tool0\WObj:=wobj_weld;  
ArcLEnd *, v1000, seam1, weld1, fine, tool0\WObj:=wobj_weld;  
MoveJ *, v1000, z50, tool0\WObj:=wobj_weld;  
MoveJ *, v1000, z50, tool0\WObj:=wobj_weld;  
ArcLStart *, v1000, seam1, weld1, fine, tool0\WObj:=wobj_weld;  
ArcLEnd *, v1000, seam1, weld1, fine, tool0\WObj:=wobj_weld;  
MoveJ *, v1000, z50, tool0\WObj:=wobj_weld;
```

## Fifth layer

```
PROC haikal5()  
MoveJ *, v1000, z50, tool0\WObj:=wobj_weld;  
MoveJ *, v1000, z50, tool0\WObj:=wobj_weld;  
ArcLStart *, v1000, seaml, weldl, fine, tool0\WObj:=wobj_weld;  
ArcLEnd *, v1000, seaml, weldl, fine, tool0\WObj:=wobj_weld;  
MoveJ *, v1000, z50, tool0\WObj:=wobj_weld;  
MoveJ *, v1000, z50, tool0\WObj:=wobj_weld;  
ArcLStart *, v1000, seaml, weldl, fine, tool0\WObj:=wobj_weld;  
ArcLEnd *, v1000, seaml, weldl, fine, tool0\WObj:=wobj_weld;  
MoveJ *, v1000, z50, tool0\WObj:=wobj_weld;  
MoveJ *, v1000, z50, tool0\WObj:=wobj_weld;  
ArcLStart *, v1000, seaml, weldl, fine, tool0\WObj:=wobj_weld;  
ArcLEnd *, v1000, seaml, weldl, fine, tool0\WObj:=wobj_weld;  
MoveJ *, v1000, z50, tool0\WObj:=wobj_weld;  
MoveJ *, v1000, z50, tool0\WObj:=wobj_weld;  
ArcLStart *, v1000, seaml, weldl, fine, tool0\WObj:=wobj_weld;  
ArcLEnd *, v1000, seaml, weldl, fine, tool0\WObj:=wobj_weld;  
MoveJ *, v1000, z50, tool0\WObj:=wobj_weld;  
ENDPROC
```



اونيورسيتي تيكنيكل مليسيا ملاك

UNIVERSITI TEKNIKAL MALAYSIA MELAKA